

**EC Access to Research Infrastructures Action  
of the Improving Human Potential Programme**



# **6<sup>th</sup> European NMR Large Scale Facilities User Meeting 2002**

**October 17 - 20, 2002, Montecatini Terme, Italy**

## **The Bio-NMR EC Research Infrastructures**

**PARABIO - Florence, IT**  
**SONNMRLSF - Utrecht, NL**  
**UNIFRANMR - Frankfurt, D**  
**WnmrC - Wageningen, NL**

## **Breakthrough in NMR of paramagnetic proteins**

*Ivano Bertini*

The Florence infrastructure is specialized in the investigation and structural characterization of metalloproteins and in particular of paramagnetic systems. As far as the paramagnetic molecules are concerned, the Florence infrastructure represents a place where the frontiers of paramagnetic molecules are debated. From the discussion of the paramagnetic contribution to the dynamic frequency shift to the characterization of paramagnetic based constraints for solution structure determination; from the understanding of the electron relaxation theory to the protocols for solution structure determination.

## **Recent Developments and Achievements of the Frankfurt University Large Scale Facility for Biomolecular MR**

*Heinz Rüterjans*

The LSF Frankfurt has established solid state NMR equipment for determining structures of membrane bound peptides and proteins. In addition, high field EPR (also ENDOR and ESEEM) will be offered for studying functional properties of proteins containing paramagnetic centres. For the investigation of solution structures of proteins or nucleic acids cryoprobe technology (for 600 and 800 MHz) is available as well as a 900 MHz NMR spectrometer which is supposed to be operational at the end of October 2002. In particular the dynamics of protein structures either in native or denaturated or even in intermediate states can be studied with the expertise of the Frankfurt LSF. For isotope labelling of proteins UNIFRANMRLSF has established a cell free expression system. Computer programs for the processing and evaluation of NMR data have been developed which are offered to potential users. Some of the results of recent projects performed at the LSF Frankfurt will be presented.

## New developments at the Utrecht SONNMR Large Sacle Facility

*Robert Kaptein*

A survey will be given of the projects that are going on at the SONNMR Large Scale Facility. Recent results obtained by the Utrecht group will also be presented, in particular with respect to protein-DNA interaction in the lac repressor system.

## Multi DARTS approaches.

*Henk Van As*

Laboratory of Biophysics and Wageningen NMR Centre, Wageningen University, Dreijenlaan 3, 6703 HA Wageningen, The Netherlands

In this contribution recent developments obtained at Wageningen NMR Centre (WNMRC) will be highlighted. In addition to progress made in LC-NMR (see contribution by De Waard et al on Saturday, October 19) we also developed a number of methods to discriminate chemically identical nuclei in different compartments or geometries. Both (low field) pulsed field gradient NMR and relaxation time measurements are widely used to probe the molecular displacements of liquid molecules and the geometry of the microstructures containing them in (multicompartment) porous and biological systems. Combined Diffusion or Displacement And Relaxation Time measurements (T2, T1 or both) allow to separate signals into a set of multicompartmental sources.

In non-imaging mode differences in relaxation time behaviour can be used for Diffusion or Displacement Analysis by Relaxation Time Separation (DARTS) (1). The interpretation can be supported by a number of PFG-CPMG Diffusion And Relaxation Time Simulations (DARTS). Recently, a fast two-dimensional Laplace inversion method has been presented to represent such 2D data sets in correlation spectra, including information on exchange (3).

In imaging mode, the S/N per pixel is in general too low to explore the differences in relaxation time directly. However, if the relaxation data is combined with displacement information multi-compartment information can be obtained even for a single pixel. This will be illustrated by imaging of water transport processes in plants and a biomat. However, the methods are generally applicable.

### References

- <sup>1</sup>van Dusschoten D, de Jager PA, Van As H. 1995. Extracting diffusion constants from echo-time-dependent PFG NMR data using relaxation-time information. *J. Magn. Reson. A* 116: 22-28.
- <sup>2</sup>van der Weerd L, Melnikov SM, Vergeldt FJ, Novikov EG, Van As. H. 2002. Modelling of self-diffusion and relaxation time NMR in multi-compartment systems with cylindrical geometry. *J. Magn. Reson.* 156, 213-221.
- <sup>3</sup>Song Y-Q, Hurlimann MD, Flaum M, Frulla P, Straley C. 2002. T1-T2 correlation spectra obtained using fast two-dimensional Laplace inversion. *J. Magn. Reson.* 154, 261-268.

## SPINS: An Integrated Approach to Automated Analysis of Protein NMR Structures

*G.T. Montelione, M.C. Baran, Y.J. Huang, H.N.B. Moseley, G. Sahato, D. Snyder, and R. Tejero*

Modern protein NMR spectroscopy laboratories have a rapidly growing need for an easily queried local archival system of raw experimental NMR datasets and intermediate results generated in the process of spectral analysis. SPINS (Standardized ProteIn Nmr Storage) is an object-oriented relational database that provides facilities for high-volume NMR data archival, organization of analyses, and dissemination of results to the public domain BioMagResBank (BMRB). The current version of SPINS coordinates the process from data collection to validation and BMRB deposition of raw NMR data and resonance assignments by standardizing and integrating the storage and retrieval of these data in a local laboratory file system. The SPINS graphical user interface (GUI) integrates several independent programs for NMR spectral processing (e.g., NMRPIPE), spectral peak picking (e.g. SPARKY), peak list editing and registration (e.g., AutoPeak), automated analysis of backbone resonance assignments (e.g., AutoAssign) determination of secondary structures for NOESY data (e.g., AutoStructure), validation of chemical shifts, and submission of fid and chemical shift data to the BMRB. This presentation will provide an overview of SPINS, a description of its implementation in Oracle, and an outline of future plans for the SPINS project within the context of the Northeast Structural Genomics Research Consortium, a NIH-funded pilot project in Structural Proteomics.

## Automated Structure Calculation of Proteins from NMR data

*W. Gronwald, B. Ganslmeier, S. Moussa, J. Trenner, A. Nassar, R. Kirchhöfer, K.-P. Neidig and H. R. Kalbitzer*

The reliable automated structure calculation from NMR data is the ultimate goal of the program AUREMOL newly developed by us. It is designed for a top-down strategy with the aim to obtain a three-dimensional structure from a minimum of NMR data using information from additional sources. It contains all necessary tools for evaluation and representation of multidimensional NMR data and can also present three-dimensional structures of proteins. Automated assignment of NOESY spectra is a prerequisite for automated structure determination of biological macromolecules. With the program KNOWNOE contained in AUREMOL we present a novel, knowledge based approach to this problem. KNOWNOE is devised to work directly with the experimental spectra without interference of an expert. Besides making use of routines already implemented in AUREMOL, it contains as a central part a knowledge driven Bayesian algorithm for solving ambiguities in the NOE assignments. These ambiguities mainly arise

from chemical shift degenerations which allow multiple assignments of cross peaks. Using a set of 1126 structurally independent protein structures, statistical tables in the form of atom-pairwise volume probability distributions (VPDs) were derived. VPDs for all assignment possibilities relevant to the assignments of interproton NOEs were calculated. With these data for a given cross peak with  $N$  possible assignments  $A_i$  ( $i = 1, \dots, N$ ) the conditioned probabilities  $P(A_i, a | V_0)$  can be calculated that the assignment  $A_i$  determines essentially all ( $a$ -times) of the cross peak volume  $V_0$ . An assignment  $A_k$  with a probability  $P(A_k, a | V_0)$  higher than 0.8 is considered transiently as unambiguously assigned. With a list of unambiguously assigned peaks a set of structures is calculated. These structures are used as input for a next cycle of iteration where a distance threshold  $D_{max}$  is dynamically reduced. When starting from a sufficiently well-defined homology structure or a structure obtained from KNOWNOE (3) a generalized threshold accepting algorithm can find initially missing assignments from the NOESY spectra only. Convergence and almost complete assignment can be obtained even when up to 30 % of the basic sequential assignment is not available at the beginning. For obtaining a more reliable fit to the experimental data a T2-calculation allowing for various modes of internal motion was incorporated. Multiplet splitting by J-coupling on the basis of the weak coupling approximation can also be included into the spectral simulation. We can show that in the cases tested this method works equally well or even better than an human expert since it avoids the bias introduced by the non-random distribution of unequivocally assignable NOE-contacts.

### References

1. Schulte, A. C., Görler, A., Antz, C., Neidig, K.-P. & Kalbitzer, H. R. (1997) *J. Magn. Reson.* 129, 165-172.
2. Görler, A. & Kalbitzer, H. R. (1997) *J. Magn. Reson.* 124, 177-188.
3. Gronwald, W., Moussa, S., Elsner, R., Jung, A., Ganslmeier, B., Trenner, J., Kremer, W., Neidig, K.-P., & Kalbitzer, H. R. (2002) *J. Biomol. NMR*, in press.

## High resolution MRI in the mouse heart in vivo

*A. Haase*

MR imaging (MRI) is an important tool in medical diagnosis and *in vivo* animal research. However, cardiovascular applications are less often possible due to the limits of MRI regarding spatial and time resolution. This has recently changed with the development of high speed MRI techniques and MR scanners having very high magnetic field strengths. Especially, cardiovascular studies in small animals, like mice became feasible using MRI.

Most of MRI experiments in mice were done in horizontal bore magnets having field strengths from 4.7 T to 11.7 T (and recently 17.6T). High speed imaging (echo-planar- and FLASH imaging) is applied in combination with ECG-triggering. The typical spatial resolution amounts to 0.1 mm. ECG-triggered 2D- and 3D-movies of a beating mouse heart in vivo can be acquired with a time resolution of a few milliseconds.

In all cases, the image contrast can be optimized to give an excellent delineation of different anatomical regions, like the ventricles, the myocardium, the lung and the blood vessels, including vessel walls (at least in large vessels, like the aorta). From these data sets, a 3D-image of the coronary artery tree can be visualized. On the basis of these MRI movies, the calculation of functional data is possible, like the cardiac output, ejection fraction, stroke volume, myocardial volume, wall diameters, etc. Additional MRI techniques also quantify the blood flow velocity and velocity profiles in blood vessels (aorta and large coronary arteries). MRI techniques are also available to measure the perfusion in the myocardium.

All these techniques have been optimized for the application in mice and are being used in different animal models, including transgenic mouse models.

A wide area of further MR studies is MR spectroscopy to detect metabolic information. Here, high energy metabolites and reaction rates can be studied using  $^{31}\text{P}$ -,  $^{13}\text{C}$ - and  $^1\text{H}$ -MR-spectroscopy. Since the metabolites have a small in vivo concentration, the spatial resolution is limited and the measuring time is long. Many applications of MR spectroscopy have been described in excised organs, but in vivo experiments are limited until now.

The advent of MR scanners of very high magnetic field strengths, like 17.6 T will dramatically change this situation. Here, the signal-to-noise ratio is increased which will reduce the measuring times. So, in one experimental session, the anatomy, the function and metabolic information can be measured non-invasively in a living mouse.

The presentation will review the present state of MRI technology and will demonstrate applications to cardiovascular mouse models.

## In-cell NMR Spectroscopy

*Zach Serber and Volker Doetsch*

The recent development of "in-cell NMR" techniques has demonstrated that NMR spectroscopy can be used to characterize the conformation and dynamics of biological macromolecules inside living cells. We show that labeling of proteins with  $^{15}\text{N}$  can be achieved with minimal background from bacterial proteins. We compare several different protocols and media and demonstrate that the over expression level is the most critical parameter. Virtually background-free in-cell NMR spectra, however, can be obtained by amino-acid type selective labeling. We further demonstrate that this selective labeling strategy can also be used for very efficient backbone assignment for in vitro samples. In addition we present new labeling procedures for  $^{13}\text{C}$ -labeling of selective proteins in the cytoplasm which can overcome the problem of high background from cellular molecules. This labeling strategy can also be used for studying large proteins in the bacterial cytoplasm. Finally, we will present applications of these in-cell NMR labeling techniques that include investigation of the dynamics of proteins and drug-protein interactions in the cytoplasm. In these experiments we demonstrate that differences in the dynamics between the intracellular and the in vitro forms of proteins can exist. In particular, backbone nitrogen spins of the metal binding loop of the small bacterial protein NmerA relax faster inside the bacterial cytoplasm than in an in vitro sample. We will discuss models that can explain these results.

## Probing plant metabolism with NMR

*R.G. Ratcliffe*

Analytical methods for probing plant metabolism have taken on renewed significance in the era of functional genomics and metabolic engineering. NMR spectroscopy is a major contributor to this endeavour, providing insights into the integration and regulation of metabolism through a combination of in vivo and in vitro measurements. Thus NMR can be used to identify, quantify, and localize metabolites, to define the intracellular environment in which metabolism takes place, and to explore metabolic pathways and their operation. These applications will be reviewed, with particular reference to the important role of NMR in pathway delineation and metabolic flux analysis. It will be concluded that NMR provides a versatile method for determining the metabolic phenotypes of wild type, mutant and transgenic plants.

## Quantification and correlation of magnetic resonance imaging and immunohistopathology of inflammatory and demyelinating lesions in MOG-induced EAE in common marmosets.

*Jan Bauer, Erwin Blezer, Herbert Brok and Bert Hart*

Multiple sclerosis (MS) is a chronic inflammatory demyelinating disease of the human central nervous system (CNS). The pathological hallmark of MS are lesions with a variable degree of inflammation, demyelination, axonal destruction and gliosis. Experimental autoimmune encephalomyelitis (EAE) is widely employed as an animal model to study the etiopathogenesis of MS and we have shown with qualitative MRI that brain lesions developing in EAE-affected common marmoset, induced by immunization with myelin/oligodendrocyte glycoprotein (MOG), resemble those in MS. The present study documents the application of high resolution (4.7 T), quantitative in vivo MRI for the investigation of brain lesion formation in this model. The different pathophysiological processes of lesion formation were monitored with magnetization transfer ratio (MTR) imaging, Gadolinium enhanced T1W imaging (for blood brain barrier integrity) and quantitative relaxation time imaging. Finally the characteristics (lesional age, inflammation, demyelination, edema, axonal loss) of the different lesions are determined by immunohistochemistry on paraffin sections and correlated to the MRI images. These studies may help to understand how specific MRI characteristics reflect specific pathophysiological changes in the brain.

## Dynamic Frequency Shift in paramagnetic proteins

*H. Desvaux*

Dynamic Frequency Shifts correspond to imaginary contributions of relaxation to the spin dynamics. These terms, generally small, are difficult to measure, since their contributions lead to periodical time dependence and consequently superimpose to the classical static Hamiltonian terms as the isotropic chemical shifts or the scalar couplings. However by the intrinsic relaxation nature of DFS, their existence depends on the pulse sequence. For instance, DFS is present when one considers the decay of a transverse component (classical T2 measurement) but DFS is absent when the decay is studied in the presence of an rf irradiation (T1<sub>rho</sub> type experiment). This remark is a clue to design pulse sequences for measuring DFS. On a structural or dynamic point of view, DFS terms correspond to the dispersive part of spectral densities. As a consequence, these terms are expected to be more sensitive to fast motions than relaxation rates. Finally since these two terms result from the same physical mechanisms, the interpretation of their relative magnitudes should agree. DFS in bio-molecular systems have currently risen little interest by their small magnitudes and the difficulties to measure them. However in the case of paramagnetic proteins, they might prevent accurate determinations of residual dipolar couplings since they exhibit the same dependence on the static magnetic field B<sub>0</sub>. Moreover in these systems, a debate remains on the correct expression of the imaginary component of the cross-correlated cross-relaxation between transverse one- and two-spin coherences which involves the Curie electronic spin. Indeed different experiments tend to prove that the ratio of the imaginary to real components is not the expected one. In this presentation, after recalling the properties of DFS, we shall describe the nature of this theoretical difficulty as well as experimental procedures developed for measuring this DFS in the calcium binding protein, where one of the two Calcium ions has been chemically exchanged by a lanthanide ion. The consequence of the presence of DFS on the structure refinement against RDCs will be discussed.

## NMR and LC-SPE-NMR in Wageningen.

*Pieter de Waard, Audrius Pukalskas, Vitalya Povilaityte, Mirjam A. Kabel*

LC-NMR is a hyphenated analytical technique combining high performance liquid chromatography (HPLC) as separation method with NMR as structural elucidation method. It has proven to be a powerful method for analysis of unknown compounds in mixtures.

So far there were three modes of operation in LC-NMR:

- On flow mode, the simplest method. NMR spectra are recorded continuously during elution of the column. Sensitivity and solvent suppression during gradients are a problem.
- Stop flow and time slicing. The elution is stopped to get a better sensitivity. Disadvantage is the resulting diffusion in the column.
- Peak sampling or loop storage. Peaks are stored in loops and can be measured later.

As an example of the use of LC-NMR in loop storage mode, a study to determine the location of O-acetyl substituents in xylo-oligosaccharides is shown. Due to acetyl migration after purification of samples, LC-NMR is the only way to get NMR spectra of pure compounds.

The latest development is the usage of the Solid Phase Extraction (SPE) system as interface between LC and NMR. After separation the peaks of interest are trapped on individual SPE cartridges. The peaks are dried and transferred with a suitable (deuterated) solvent into the NMR flow probe.

The major advantages of the LC-SPE-NMR technique are:

- Chromatographic separation can be done with cheap non-deuterated solvents or and even with additives which are not compatible with NMR spectroscopy.
- The complete sample is eluted in a small volume (< 50 µl) of deuterated liquid from the SPE cartridge. Due to this concentration effect a substantial increase in sensitivity is observed, especially for broader peaks. Solvent suppression is not needed anymore.
- By multiple collection from subsequent separations of the same sample the amount and concentration can be further increased, improving the sensitivity even more.

Examples of the use LC-SPE-NMR are shown. Combination with another hyphenated technique, detection of radical scavenging compounds based on reduction of 2,2-diphenyl-1-picrylhydrazyl radical (DPPH), resulted in LC-SPE-NMR-DPPH.

## Calmodulin regulates transcription via a novel mode of Calmodulin target interaction. Structure and dynamics of the dimeric CaM:SEF2-1mp complex.

Goran Larsson<sup>1</sup>, Juergen Schleucher<sup>1</sup>, Juha Saarikettu<sup>2</sup>, Natalia Sveshnikova<sup>2</sup>, Janusz Zdunek<sup>1</sup>, Thomas Grundstrom<sup>2</sup>, and Sybrene S Wijmenga<sup>1,3</sup>

<sup>1</sup>Medical Biochemistry and Biophysics, Umea University, Umea, Sweden

<sup>2</sup>Molecular Biology, Umea University, Umea, Sweden

<sup>3</sup>Biophysical Chemistry, University of Nijmegen, Nijmegen, The Netherlands  
email: sybrenw@sci.kun.nl

Calmodulin (CaM) is a Ca<sup>2+</sup> sensor protein that regulates numerous cellular processes via specific CaM:protein interactions. More than 100 targets are known, among them the CaM inhibited basic-Helix-Loop-Helix (bHLH) transcription factors SEF2-1 (E2-2), E12 and E47. CaM binds as a dimer to the basic regions of the dimeric bHLH in a highly specific manner and with dissociation constant in the nano-molar range.

We report the solution structure and dynamics of the 38 kDa complex formed by CaM with the dimeric binding domain of SEF2-1. This dimeric binding domain was mimicked via a SEF2-1 mimicking peptide, SEF2-1mp, consisting of the two basic regions of SEF2-1 connected via an S-S bridge. The structure was derived based on classical NMR constraints complemented with global structure information derived from <sup>15</sup>N-relaxation measured at two magnetic fields. The dimeric target binds inside a figure-eight-shaped CaM dimer via multiple-binding alternatives. The CaM:CaM interaction is evident from intermolecular CaM NOEs, while the multiple-binding modes follow from mutually exclusive CaM:SEF2-1mp NOEs. Multiple-binding alternatives are also demonstrated by the gradual decrease in CaM affinity upon sequential mutagenesis of the related E12 protein, and by the complex binding curves observed by fluorescence binding studies.

To further characterize this unusual CaM:target interaction, we investigated the dynamics of this via <sup>15</sup>N-relaxation data measured at two fields and two temperatures. Within the complex, the two N-terminal and two C-terminal domains of the calmodulin dimer undergo wobbling motions characterized by an effective correlation time and squared-order parameter of ca. 2.0 ns and 0.75, respectively. Moreover, residues with significant exchange broadening are found. They have similar exchange times (ca. 50 microseconds) and are grouped in structural 'hotspots'. These features show that the exchange between the multiple-binding alternatives of SEF2-1mp occurs via large-scale internal motions on both the nanosecond and microsecond time scale.

This new type of CaM:target binding is essentially different from lock-and-key and induced-fit binding. We denote it as 'flexchange binding' because it is characterized by context dependent (e.g. dimerization) binding via multiple alternatives.

## NMRD studies of some Ni(II), Mn(II) and Gd(III) complexes in aqueous solution

Jozef Kowalewski, Tomas Nilsson and Danuta Kruk

NMRD profiles have been measured between less than 1 mT and 18.8 T for several Ni(II) complexes with macrocyclic ligands, representing different coordination geometries. The profiles share in all cases certain characteristic features. The relaxation rate at low field is approximately constant and increases sharply at higher field, starting at around 1 T. The NMRD profiles are interpreted using a general theory ("slow motion theory") for nuclear spin relaxation in paramagnetic systems in solution, valid also beyond the Redfield limit. The resulting parameters (metal-proton distance, transient and static zero-field splitting, distortion correlation time) can be rationalised in terms of structural features of the complexes.

For complexes of Gd(III) and Mn(II) of interest as MRI contrast agents, the same theoretical approach for analyzing the data is not really feasible. Simpler methods, based on the Redfield theory, have therefore been developed and applied for the interpretation of NMRD profiles from literature. These methods function best for large complexes with long rotational correlation times, but some progress has also been made for low-molecular weight systems.

## Automated liquid-flow NMR screening of RNA-targeting peptides and ligands.

*Frédéric Dardel and Carine Tisné*

RNA is an important therapeutic target in the context of infectious diseases : About half of the antibiotics currently used for treating bacterial infections in man actually target different parts of ribosomal RNA (e.g. macrolides, aminoglycosides, tetracyclins, lincosamides, streptogramines...). The genome of a number of human viruses, including the AIDS causative agent, HIV-1, is composed of RNA which often folds into complex 2D and 3D structures involved in key events in the viral cycle (encapsidation, replication, activation, splicing...). It is therefore of great interest to investigate a general strategy for the isolation of specific RNA ligands which might interfere with these processes.

We use high-field NMR spectroscopy to identify ligands which bind to a given RNA. The target RNA is enriched with stable isotopes ( $^{15}\text{N}$ ) and the resonances corresponding to the imino groups are monitored by 2D heteronuclear correlation spectroscopy (HSQC).

In order to be efficient, this technique requires (1) a reasonable throughput and (2) an "optimized" compound library to be screened :

We have chosen automated liquid flow NMR to meet the first of these two requirements, which additionally reduces the amount of required sample. Using our procedure, up to 50-100 screens/day can be performed, without human intervention.

As a combinatorial library, we use an optimized set of hexapeptides. This small scale library has been designed in silico to satisfy a number of criteria : solubility, isoelectric point (all peptides are slightly to moderately basic), non-redundancy at the di- and tripeptide level. We have also used aminoacid similarity matrices (BLOSUM) to obtain an "optimal sampling" of the tetrapeptide space by minimizing the pairwise similarity between any two peptides in our library. In addition to this "RNA-specific" peptide library , we also use screen a small set of organic molecules likely to interact with nucleic acids (polyamines, intercalating agents, heterocyclic bases...) which could be subsequently combined with candidate peptides to obtain high affinity ligands. Indeed, there exists a naturally occurring RNA-binding antibiotic, edeine, which is such a combination of a pentapeptide linked to a polyamine : spermidine.

An application to the HIV-1 reverse transcription initiation primer will be presented.

## Bacterial energy metabolism during bacteriophage replication: a $^{31}\text{P}$ NMR study

*Kaja Gnezda, Cor Dijkema, David Stopar*

Intracellular bacteriophage replication produces stress for the host bacterial cell. It induces changes in the cell physiology and eventually leads to cell death. It remains to be elucidated whether the replicating bacteriophage influences the homeostasis of the cellular energy metabolism. To approach this issue,  $^{31}\text{P}$  NMR spectra were obtained of cellular extracts of wild-type marine *Vibrio* isolate in which the bacteriophage replication is either induced or not induced by the specific antibiotic. To assign peaks in the obtained spectra to known metabolites of cellular energy metabolism, 27 standard phosphorylated compounds of known concentrations were added to the cellular extracts, namely glycolytic sugar phosphates, nucleotides (NTP, NDP, NMP) and cofactors (NAD, FAD). Preliminary analysis of  $^{31}\text{P}$  NMR spectra of control and induced cultures shows that replicating bacteriophage significantly influences the quantitative ratios of some phosphorylated metabolites of cellular energy metabolism.

## Cellular Retinol-binding Protein I: an NMR Study of its Structural Features and Stability

*Lorella Franzoni<sup>1</sup>, Christian Lücke<sup>2</sup>, Davide Cavazzini<sup>3</sup>, Alberto Spisni<sup>1</sup>, Gian Luigi Rossi<sup>3</sup> and Heinz Rüterjans<sup>2</sup>*

<sup>1</sup>Department of Experimental Medicine - Section of Chemistry and Structural Biochemistry, University of Parma, 43100 Parma, Italy;

<sup>2</sup>Institute of Biophysical Chemistry, G.W. Goethe University of Frankfurt, 60439 Frankfurt, Germany;

<sup>3</sup>Department of Biochemistry and Molecular Biology, University of Parma, 43100 Parma, Italy.

Cellular retinol-binding proteins (CRBPs) play important roles in regulating uptake, transport, storage, and metabolism of vitamin A. The four mammalian CRBP types identified so far appear to possess rather distinct tissue distribution and physiological functions. Among them, CRBP type I (134 residues, 15.7 kDa) forms the most stable complex with retinol and is widely expressed in various tissues. Like in the case of other members of the intracellular lipid-binding protein (i-LBP) family, the mechanism of ligand uptake and targeted release remains to be clarified.

In our recent work, the solution structure and backbone dynamics of CRBP have been determined in the apo and holo-form (1). To further investigate the structural features and conformational stability of the protein, a series of multidimensional NMR experiments were recorded under different solution conditions using non-labeled and uniformly <sup>15</sup>N-enriched protein samples. Hence, measurements were carried out either at acidic pH or in the presence of increasing amounts of methanol. In addition, hydrogen/deuterium (H/D) exchange experiments were performed.

The results will be discussed in comparison with other members of the i-LBP family.

### References

(1) Franzoni, L., Lücke, C., Pérez, C., Cavazzini, D., Rademacher, M., Ludwig, C., Spisni, A., Rossi, G.L. and Rüterjans, H. (2002) *J. Biol. Chem.* 277, 21983-21997.

### Acknowledgements

Supported by grants from CNR, "Target Project on Biotechnology", and MIUR (Italy). The European Large Scale Facility for Biomolecular NMR at the University of Frankfurt (Germany) is gratefully acknowledged for the use of its equipment.

## A CP-MAS <sup>13</sup>C NMR Study On Complexation Of Cations To Soil Organic Matter

*Aleksandra Badora<sup>1</sup>, Barend van Lagen<sup>2</sup>, Adrie de Jager<sup>3</sup> and Peter Buurman<sup>2</sup>*

<sup>1</sup>Department of Agricultural Chemistry, Agricultural University of Lublin, Akademicka 15, 20-950 Lublin, Poland

<sup>2</sup>Laboratory for Soil Science and Geology, Department of Environmental Sciences, Wageningen University, P.O. Box 37, 6700 AA Wageningen, the Netherlands

<sup>3</sup>Wageningen NMR Centre and Laboratory of Biophysics, Wageningen University, P.O. Box 8128, 6700 ET Wageningen, The Netherlands

We studied metal complexation to soil organic matter by measuring both changes in T<sub>CH</sub> and T<sub>1</sub> in <sup>13</sup>C-CPMAS VCT experiments.

The experiment was carried out on NaOH-extracts of organic matter from two types of soil – two samples from a podzol (The Netherlands) and four samples from volcanic soils of the Azores Islands, which were widely different in chemical, physical and biological characteristics. All six samples were mixed separately with H<sup>+</sup>, Na<sup>+</sup>, Cu<sup>2+</sup> and Al<sup>3+</sup> chlorides to obtain different organic matter-cations complexes. The protonated SOM (solid organic matter) is used as a reference; Al is a common counter-ion in soils, which is strongly complexed and not paramagnetic; Cu is both strongly complexed and paramagnetic; and Na is only loosely bound. The protonated and saturated samples were dialysed against demineralised water and freeze-dried.

The CP-MAS <sup>13</sup>C NMR spectra of prepared samples were obtained using a Bruker AMX 300 spectrometer operating at a frequency of 75.48 MHz. The samples were spinning at 5 kHz using room temperature air for drive and bearing pressure. The Hartmann-Hahn condition was determined using glycine as a standard. The samples were measured at 13 different contact times (VCT: 0.1; 0.2; 0.5; 0.8; 1–(three times); 1.2; 1.5; 2; 3; 4; 5; 6; 7 ms) to obtain full information on cross polarization times and observed carbon. A 1000 number of scans were used pro experiment. The measurement of all protonated and saturated samples

Were performed three times in order to compare the obtained results.

The obtained spectra were sub-divided into regions: alkyl-C, O-alkyl-C, aromatic-C and carbonyl-C. A processing of the Free Induction Decay (FID) and the spectra was done using Bruker WINNMR software package version 6. A backward linear prediction of six points was used to reconstruct the start of the FID. Priori to Fourier transformation, the FID was multiplied with an exponential function producing a line broadening of 50 Hz. Spectra were phased by adjusting the zero order phase correction and a fixed first order phase factor. A sixth order baseline polynomial correction was applied [van Lagen and de Jager 2002]. For the curve fitting Win Sigma Plot by Jandel Scientific was used.

Depending on soil sample and kind of cations, different percentages of observed carbon was found. We could not measure the cross-polarization effect in the Cu-organic matter complexes in the carboxylic and aromatic regions (too short time). T<sub>1</sub> were different for the selected regions in the samples. Aluminium appears to slow down the T<sub>1</sub> compared with protonated samples. Other data are forthcoming.

### References

B. van Lagen and P.A. de Jager. 2002. Improving quantification of <sup>13</sup>C CP-MAS NMR by steady state and well-defined data processing in variable contact time experiments. *Organic Geochemistry* (submitted).

## Structure and Dynamics of the two domain protein Pin1

*Doris Jacobs, Krishna Saxena, Martin Vogtherr, Klaus Fiebig*

The peptidyl-prolyl cis-trans isomerase (PPIase) Pin1 is essential for cell cycle regulation. Pin1 (18.4 kDa) consists of a N-terminal WW domain (Pin1\_WW) which is important in substrate targeting, and a C-terminal catalytic domain (Pin1\_Cat) which is structurally homologous to the FKBP-class of PPIases.

Pin1 selectively isomerizes peptides containing phospho-Ser/Thr-Pro sequence motifs. These peptides interact not only with Pin1\_Cat but can also bind to Pin1\_WW. Selectivity is achieved by two specific phosphate binding sites located next to the active site of Pin1\_Cat and within the peptide binding epitope of Pin1\_WW. Two X-ray studies have characterized these Pin1-peptide interactions previously: the structure of a dipeptide bound to the presumed active site of Pin1 (Ranganathan et al.), and the structure of Pin1 complexed to a doubly phosphorylated peptide peptide (Verdecia et al.). Also, a  $^1\text{H}$  NMR study (Wintjens et al.) has compared the structure of free Pin1\_WW with Pin1\_WW in complex with the Cdc25 and the tau phospho-Thr peptides.

In this study we use NMR methods to address the impact of peptide binding on the two domain nature of Pin1. We have analyzed  $^{15}\text{N}$  spin relaxation data in order to compare the domain flexibility of free and of peptide bound Pin1.  $^{15}\text{N}$  NOE data clearly show two well structured domains separated by a 20 amino acids long flexible linker. Without peptide bound to Pin1, the relaxation data of the two domains must be fit separately. Thus Pin1\_WW and Pin1\_Cat tumble isotropically with average overall correlation times  $\tau_c$  of 7.7 ns and 9.7 ns, respectively. In comparison,  $\tau_c$  of Pin1\_WW alone is 4.1 ns indicating that the linker induces weak interactions between Pin1\_WW and PinCat.

The flexibility of the two domains is significantly restricted when the peptide WFYpSPR is bound to Pin1, as evidenced by the increased  $\tau_c$  of 9.5 ns for Pin1\_WW and 10.5 ns for Pin1\_Cat. Unfortunately it was only possible to 90% saturate Pin1 with the peptide. Hence extrapolating the relaxation data of Pin1\_WW to 100% saturation resulted in approximately equal  $\tau_c$ 's for both domains. Thus, the peptide-bound Pin1 tumbles isotropically as a whole molecule with a  $\tau_c$  of 10.7 ns.

To localize the interaction surface of Pin1 and the peptide we used differential chemical shift mapping employing full length Pin1 and various deletion mutants. As expected from the relaxation data the peptide not only interacts with the PinCat active site and the peptide binding site of the Pin1\_WW domain, but also is involved in interactions at the Pin1\_WW/Pin1\_Cat domain-domain interface. Hence in agreement with the relaxation data, we conclude that the peptide causes the independent Pin1\_WW and Pin\_Cat domains to interact.

### References

- Ranganathan et al. (1997) Cell, 89, 875-86.  
 Verdecia et al. (2000) Nat. Struct. Biol., 7, 639-43.  
 Wintjens et al. (2001) J. Biol. Chem., 276, 25150-6.

## The extracellular domains of the signaltransducer gp130

*Michael Pachta-Nick, Rainer Wechselberger, Nico van Nuland, Joachim Grötzinger*

Glycoprotein 130 (gp130) is a type I transmembrane protein and serves as the common signal-transducing receptor subunit of the interleukin-6-type cytokines. Whereas the membrane-distal half of the gp130 extracellular part confers ligand binding the structural and functional features of its membrane-proximal half are poorly understood. On the basis of predictions of tertiary structure, the membrane-proximal half consists of three fibronectine-type-III-like domains D4, D5 and D6. However, to gain certainty and to understand the relation between structure and function it is necessary to solve its structure, for instance by NMR spectroscopy.

We expressed the recombinant single domains D4, D5 and D6 and two constructs consisting of the coupled domains D5 and D6, D3 and D4, respectively. While the three single domains turned out to be relatively unstable particularly regarding temperature and concentration, the two double domains are easy to handle. After purification and concentration of the double domain D56 the triple resonance NMR spectra were recorded and used for the sequential assignment of this 25 kDa protein.

## Carving up a colicin: engineering of a 71 kDa protein complex for NMR

*G.R.Moore, C.Kleanthous, R.James, C.Penfold, R.Boetzel, C.MacDonald and K.Tozawa*

One of the problem areas in protein NMR is getting suitable samples of isotopically labelled protein. For small proteins  $^{15}\text{N}$  or  $^{13}\text{C}/^{15}\text{N}$  labelling is often sufficient, but for large proteins  $^2\text{H}$  labelling may also be required, though protein engineering to obtain well-behaved, and functional, fragments of large proteins is a widely used approach for generating NMR samples. Cell-free expression systems are being developed but the majority of NMR groups use microbial or insect cell expression systems, which generally require a high level of expression to be economic. His-tagged protein constructs are commonly expressed to allow use of metal-affinity columns in sample purification.

Each of the common methods referred to above have particular features that can cause unexpected problems. For example, even if the gene is expressed does the protein fold? Is it degraded in the cell? Does it bind  $\text{Ni}^{2+}$ , and if so how can it be removed? If the protein is too large for conventional  $^{13}\text{C}/^{15}\text{N}$  experiments without deuteration, has it a domain structure that can be exploited to provide smaller units for NMR? How can domains be recognised?

We have faced all these issues in our study of the complex formed by the 61 kDa colicin E9 endonuclease toxin and its 9.5 kDa inhibitor protein. The toxin is lethal to bacterial cells without the inhibitor protein, which might be thought to present some difficulties in expressing it in an active form. It consists of 3 major functional domains: the natively unfolded translocation domain, a coiled-coil receptor-binding domain, and a transition metal ion binding killing domain. We have mapped and expressed functional units of each of these in *E.coli*, as will be described.

## Studies of Proteins in the Solid State: Assignments and Tools Towards Structures

*A. McDermott*

Solid state NMR 2D spectroscopy was used to correlate carbon backbone and sidechain chemical shifts for uniformly  $^{13}\text{C},^{15}\text{N}$ -enriched microcrystalline ubiquitin. High applied field strengths, 800 MHz for protons, moderate proton decoupling fields, 80-100 kHz, and high sample spinning rates, 20 kHz, were used for 2D carbon-carbon spectroscopy to define sidechain connectivities, in collaboration with the group of Kurt Zilm at Yale University. Moderate applied field strengths, 400 MHz for protons, were used for 3D heteronuclear spectroscopy, to define site-specific connectivities. The effect of the applied field strength on the success of these methods will be discussed.

### Chromodomain proteins: From structure to function

*Peter R. Nielsen, Abarna Thiru, Daniel Nietlispach, Helen R. Mott, Juliana Callaghan, Natalia V. Murzina and Ernest D. Laue*

This lecture will outline our studies of the HP1 family of chromodomain proteins, illustrating how knowledge of the structure of the chromodomain prompted us to carry out biochemical studies of their function. The structure of HP1 and its mode of interaction with other proteins, as determined by NMR spectroscopy, will be described. The combined structural and biochemical data now suggest hypotheses of how these proteins might function, which can be tested in future experiments.

### Molecular recognition during spliceosome assembly

*Philipp Selenko, Ana C. Messias, Remco Sprangers, Gunter Stier, Zhihong Liu, Ingrid Luyten, Matthew Bottomley, Katia Zanier, Michael Sattler*

At the onset of spliceosome assembly sequences at the 3' splice site are recognized by the splicing factors SF1 and U2AF which interact with each other and bind cooperatively to the intron RNA. SF1 recognizes the branch site sequence UACUAAC, while U2AF binds to the adjacent polypyrimidine tract. An N-terminal region of SF1 mediates binding to the C-terminal, third RNA binding domain (RBD3) of U2AF65. This interaction is modulated by phosphorylation of Ser-20 of SF1.

We have used heteronuclear multidimensional NMR spectroscopy to determine the structural bases for the intron RNA recognition by SF1 and the SF1/U2AF65 interaction. The structural data are combined with mutational analysis of the molecular interactions and provide a detailed view of protein/protein and protein/RNA interactions involving the two splicing factors.

## Inferential structure determination

*Michael Habeck, Wolfgang Rieping, Michael Nilges*

Structure determination from NMR data is an inference problem: the measured quantities are noisy and mostly incomplete and therefore insufficient to determine the structure uniquely. The objective of structure determination is to explore all regions of conformational space compatible with the incomplete experimental information at hand. Inferential Structure Determination infers conformations from the experimental evidence and background information. This is achieved by Bayes' Theorem: a statistical model explaining the experimental evidence is combined with the prior distribution implementing background knowledge to yield the posterior density which represents the full knowledge about the target structure. A Maximum Entropy distribution derived from a standard molecular dynamics force field is used to incorporate physical a priori knowledge. Cross-relaxation rates from NOESY-experiments depend on molecular conformation but cannot be used directly for structure determination: spectra have to be "calibrated" and additional parameters, e.g. "force constants", must be introduced to relate structural parameters, most typically distances, to measured peak volumes. These auxiliary parameters are not measurable. In standard approaches, they are fixed to reasonable values, thus assumed as known. In the Bayesian view both atomic coordinates and "nuisance parameters", necessary only for data modelling, are treated as unknown. Their joint posterior is estimated from the experimental data; integration over all nuisance parameters yields the marginal posterior-distribution defined on the full conformational space.

We present the first implementation of this principle for structure determination of macromolecules from NMR data. It is shown that the high-dimensional joint-posterior can be simulated for medium-sized proteins by means of a combined Hybrid-Monte-Carlo/Gibbs-Sampler. To construct a fast mixing and ergodic Markov-chain, simulation in a generalized ensemble, embedded in a parallel Replica-Monte-Carlo scheme, is found to be essential. There are many benefits in using a rigorous statistical approach to structure determination. Since the various sources leading to uncertainties in structural coordinates are modelled explicitly, statistically meaningful variances and correlations of atomic coordinates can be calculated. Quality and consistency of the experimental data is assessed by means of confidence intervals. In the probabilistic framework, all nuisance parameters involved are given a strict and intelligible interpretation.

## G-Protein coupled receptors studied by high resolution NMR spectroscopy

*A. Asnastasiadis-Pool and H. Schwalbe*

The mammalian photoreceptor rhodopsin is a prototypic member of the superfamily of cell surface G-protein coupled receptors (GPCR). GPCR genes correspond to 3% of all genes in humans. Bovine rhodopsin contains 348 amino acids. Rhodopsin is composed of three domains, the cytoplasmic (CP), the transmembrane (TM), and the intradiscal (ID) domain. 11-cis retinal, the inverse agonist, binds in a pocket in the TM domain and is linked to Lys296 in helix VII via a protonated Schiff base. Light activation causes isomerization of the retinal to the all-trans form leading to helix movements in the TM domain, which bring about a conformational change in the CP domain. Protein-protein interactions required for sensitization and desensitization in the visual system are thus initiated.

The isomerization of the retinal from 11-cis to all-trans occurs in less than 200fs. 11-cis retinal is the universal chromophore in vision of vertebrates and invertebrates. Upon isomerization of 11-cis retinal to all-trans retinal, a number of transient intermediates are formed which can be trapped at low temperatures.

The conformational changes of the different states of rhodopsin are investigated by photo-CIDNP experiments. Membrane compatible dyes are being developed for photo-CIDNP experiments.

## Assembly of Protein Subunits within the Stromal Ridge of Photosystem I. Structural Changes between Unbound and Sequentially PS I-bound Polypeptides and Correlated Changes of the Magnetic Properties of the Terminal Iron-Sulfur Centers.

*Mikhail L. Antonkine, Patrick Jordan, Petra Fromme, Norbert Krauss, John H. Golbeck and Dietmar Stehlik*

The X-ray structure of Photosystem I (PS I) was recently solved at 2.5 Å resolution (PDB entry 1JB0). It contains a structural model for stromal subunits PsaC, PsaD and PsaE, which comprise the “stromal ridge” of PS I. In a separate set of studies the three-dimensional solution structures of unbound, recombinant PsaC (PDB entry 1K0T) and PsaE (PDB entries 1QP2 and 1PSF) subunits were solved by NMR. The PsaC subunit of Photosystem I (PS I) is a small (9.3 kDa) protein that harbors binding sites for two [4Fe-4S] clusters FA and FB, which are the terminal electron acceptors in PS I. Comparison of the NMR structure of unbound PsaC in solution with the structure of PsaC in PS I-bound state clearly reveals significant differences between that occur upon binding of PsaC to PS I. Changing biochemical and magnetic properties of [4Fe-4S] centers FA and FB correlate to changes in the protein structure of PsaC. They are also influenced by the presence or absence of PsaD and are studied in the three assembly stages: PsaC (free), PsaC (only), PsaC (PS I). Unbound, recombinant PsaD was also investigated by NMR and found to have no stable three-dimensional structure in solution with only a few elements of the secondary structure. This is quite different from PS I-bound PsaD which has a well defined three-dimensional structure. Thus binding of PsaD to PS I is accompanied by formation of secondary structure elements of its parts and tertiary structure of the protein as a whole. The three dimensional structure of PsaE is very similar in solution and in PS I-bound forms. The changes in PsaC and PsaD structures are caused by the sequential formation of multiple networks of contacts between the polypeptides of the stromal ridge and also between them and PsaA/PsaB core polypeptides. The aim of this work is to understand how formation of these contacts is related to the structural changes in the proteins involved and to propose a model for assembly of the stromal ridge of PS I based on the analysis of contacts and comparison between NMR structures of unbound stromal subunits in solution and their structure in PS I-bound state.

---

### **Solution structure of CopC: a cupredoxin-like protein involved in copper homeostasis**

*Fabio Arnesano, Lucia Banci, Ivano Bertini, Andrew R. Thompsett*

The solution structure of CopC, a protein involved in copper homeostasis, has been obtained. The fold is a Greek key beta-barrel similar to that of functionally unrelated blue-copper proteins but with important structural variations. The protein binds one equivalent of copper(II) with relatively high affinity and it contains a cluster of conserved residues (His1, Glu27, Asp89 and His91) which could form a water accessible metal binding site. The structure also reveals a loop containing the M(X)nM motif which is present in a number of proteins also involved in copper homeostasis. The present structure represents a link between copper trafficking proteins and cupredoxins. Within a structural and genomic analysis, the role of CopC in copper trafficking is proposed.

---

### **Paramagnetic NMR constraints in heme proteins**

*Michael Assfalg, Giuseppe Battaini, Ivano Bertini, Claudio Luchinat, Paola Turano*

Iron(II) and iron(III) are the most commonly encountered oxidation states of iron in heme proteins. With the exception of low-spin iron(II), all the other forms are paramagnetic. Iron(III) low-spin  $S=1/2$  and iron(II) high-spin  $S=2$  possess sizable magnetic anisotropy. As an effect nuclei within a certain shell around the metal ion experience pseudocontact shifts. Moreover, the magnetic anisotropy leads to significant partial orientation that gives rise to measurable residual dipolar couplings. Pseudocontact shifts and residual dipolar couplings can be used as constraints for structural determination. Possible discrepancies between these two sets of constraints can be ascribed to protein mobility. The examples of iron(III) low-spin cytochrome c and iron(II) high-spin deoxy-myoglobin are discussed. Studies of the Curie dipole-dipole cross-correlation effect are in progress on high-spin iron(III) met-myoglobin.

## A CP-MAS $^{13}\text{C}$ NMR Study On Complexation Of Cations To Soil Organic Matter

*Aleksandra Badora<sup>1</sup>, Barend van Lagen<sup>2</sup>, Adrie de Jager<sup>3</sup> and Peter Buurman<sup>2</sup>*

<sup>1</sup>Department of Agricultural Chemistry, Agricultural University of Lublin, Akademicka 15, 20-950 Lublin, Poland

<sup>2</sup>Laboratory for Soil Science and Geology, Department of Environmental Sciences, Wageningen University, P.O. Box 37, 6700 AA Wageningen, the Netherlands

<sup>3</sup>Wageningen NMR Centre and Laboratory of Biophysics, Wageningen University, P.O. Box 8128, 6700 ET Wageningen, The Netherlands

We studied metal complexation to soil organic matter by measuring both changes in  $T_{\text{CH}}$  and  $T_1$  in  $^{13}\text{C}$ -CPMAS VCT experiments.

The experiment was carried out on NaOH-extracts of organic matter from two types of soil – two samples from a podzol (The Netherlands) and four samples from volcanic soils of the Azores Islands, which were widely different in chemical, physical and biological characteristics. All six samples were mixed separately with  $\text{H}^+$ ,  $\text{Na}^+$ ,  $\text{Cu}^{2+}$  and  $\text{Al}^{3+}$  chlorides to obtain different organic matter-cations complexes. The protonated SOM (solid organic matter) is used as a reference; Al is a common counter-ion in soils, which is strongly complexed and not paramagnetic; Cu is both strongly complexed and paramagnetic; and Na is only loosely bound. The protonated and saturated samples were dialysed against demineralised water and freeze-dried.

The CP-MAS  $^{13}\text{C}$  NMR spectra of prepared samples were obtained using a Bruker AMX 300 spectrometer operating at a frequency of 75.48 MHz. The samples were spinning at 5 kHz using room temperature air for drive and bearing pressure. The Hartmann-Hahn condition was determined using glycine as a standard. The samples were measured at 13 different contact times (VCT: 0.1; 0.2; 0.5; 0.8; 1–(three times); 1.2; 1.5; 2; 3; 4; 5; 6; 7 ms) to obtain full information on cross polarization times and observed carbon. A 1000 number of scans were used per experiment. The measurement of all protonated and saturated samples

Were performed three times in order to compare the obtained results.

The obtained spectra were sub-divided into regions: alkyl-C, O-alkyl-C, aromatic-C and carbonyl-C. A processing of the Free Induction Decay (FID) and the spectra was done using Bruker WINNMR software package version 6. A backward linear prediction of six points was used to reconstruct the start of the FID. Prior to Fourier transformation, the FID was multiplied with an exponential function producing a line broadening of 50 Hz. Spectra were phased by adjusting the zero order phase correction and a fixed first order phase factor. A sixth order baseline polynomial correction was applied [van Lagen and de Jager 2002]. For the curve fitting Win Sigma Plot by Jandel Scientific was used.

Depending on soil sample and kind of cations, different percentages of observed carbon was found. We could not measure the cross-polarization effect in the Cu-organic matter complexes in the carboxylic and aromatic regions (too short time).  $T_1$  were different for the selected regions in the samples. Aluminium appears to slow down the  $T_1$  compared with protonated samples. Other data are forthcoming.

### References

B. van Lagen and P.A. de Jager. 2002. Improving quantification of  $^{13}\text{C}$  CP-MAS NMR by steady state and well-defined data processing in variable contact time experiments. *Organic Geochemistry* (submitted).

## Structural and functional studies of a CspB/ssDNA complex

*Jochen Balbach and Markus Zeeb*

The cold shock protein CspB of *Bacillus subtilis* belongs to a family of proteins, which are believed to function as ‘RNA-chaperons’ by a rather unspecific binding to nucleic acids. CspB is an important model for single stranded nucleic acid binding proteins, such as translation initiation factor IF1, ribosomal proteins S1 and S17, or transcription terminator factor Rho. Only few structures of proteins in complex with ssDNA or unstructured RNA are known today.

In the present paper, we characterised the nucleic acid binding of CspB to two single stranded DNA fragments: a 25mer containing the Y-Box motif ATTGG (KD=0.4mM) and a 7mer of thymidine nucleotides (dT7, KD=15nM). NMR titration experiments revealed the residues, which are involved in the ssDNA binding. They include 8 out of the 9 aromatic residues of CspB and belong mainly to the RNP1 and RNP2 motifs. Several residues in the loops connecting  $\beta$ -strands 3 and 4 as well as 4 and 5 suggest conformational changes of the protein backbone upon binding. This was verified in the NMR structure of the protein in complex with dT7. Both loops turn about  $90^\circ$  towards the bound ssDNA fragment. All residues involved in binding have been confirmed by point mutations. An extended Lipari-Szabo relaxation analysis revealed that the backbone dynamics of the protein are not affected by the ssDNA on a sub-nanosecond time scale, but the chemical exchange contributions to the  $R_2$  rates get significantly reduced. These reduced millisecond dynamics were confirmed by decreased exchange rates of the fast exchanging amides determined by a modified NEW MEXICO method. Additional amide proton exchange experiments at different pH values reveal a significant increase of slowly exchanging protons upon complex formation. Stopped-flow fluorescence quenching experiments of all protein variants showed that a constant association rate allows CspB to map the nucleic acid for the target sequence and a strongly reduced dissociation rate facilitates tight binding to this site.

### Sub-second kinetics as monitored by stopped-flow NMR

*R. Barbieri, I. Bertini, P.J. Hore, C. Luchinat, K. Nerinovski, R. Pierattelli*

The development of procedures involving rapid mixing of reactants within an NMR tube is transforming NMR into a powerful technique for the study of a wide range of rapid processes occurring on a sub-second timescale, such as ion binding and exchange, protein folding/unfolding, etc. Spectral complexities can be dealt with by exploitation of either selective nuclear polarization (as in CIDNP experiments) or by the monitoring of isolated resonances, such as those arising from hyperfine-shifted nuclei. We present here two examples of the latter approach, aimed at the investigation of rapid processes involving the lanthanide-substituted calcium binding protein calbindin-D9k. In the first example, the calcium/cerium exchange is characterized, and a bimolecular associative mechanism is proposed, while in the second the cerium-induced refolding of the denatured protein is studied. Preliminary analysis of the data suggests a rapid uptake of the metal ion. The work was in part supported by the EC contract Transient NMR (no. HPRI-CT-1999-50006).

### Haem containing PAS domain sensor proteins

*Paul Barker and Roberta Pierattelli*

The PAS domain is a ubiquitous protein domain found in a wide variety of sensor proteins with little sequence homology. Despite having varied sensor roles and binding different cofactors, the known structures of PAS domains are remarkably similar. We are studying the properties of the E. coli Direct Oxygen Sensor (DOS) by protein engineering and NMR. This haem containing homodimeric protein is a fragment of a larger protein that also has phosphodiesterase activity that is coupled to oxygen binding to the haem iron. This oxygen binding haem centre is unusual in that dioxygen displaces a methionine ligand in a 6 coordinate ferrous haem. We are obtaining structural and dynamic information with a view to elucidating the mechanism of signal transduction between protein domains. NMR studies of the homodimer of 26kDa is a variety of oxidation and spin-states present an exciting challenge for current methodology.

## Structural basis of paxillin/FAK interaction

*I. Barsukov, J. Ellis, B. Patel, A. Prescott, G.C.K. Roberts, D. Critchley*

Integrin-mediated cell migration is fundamental to a wide variety of biological processes including embryonic development, wound healing, inflammation and metastasis. Key to cell migration is the assembly of a macromolecular complex on the cytoplasmic face of integrins which includes both cytoskeletal proteins which couple integrins to the actomyosin contractile apparatus (talin, filamin a-actinin, vinculin), and proteins that regulate the dynamic properties of cell-matrix junctions such as pp125FAK and paxillin. Both FAK and paxillin are large multidomain proteins. They can form a complex where the C-terminal FAT domain of FAK binds to the N-terminal LD-domain of the adaptor protein paxillin. The LD domain of paxillin contains five homologous LD1-LD5 motifs. Only LD2 and LD4 have significant affinity to FAK. We present NMR structural studies of FAK/paxillin interaction leading to a model of the complex. Cooperativity between LD2 and LD4 in FAK binding is discussed

## The unfolding of oxidized c-type cytochromes: the instructive case of *B. pasteurii*

*Ilaria Bartalesi, Ivano Bertini, Kaushik Ghosh, Antonio Rosato, Paola Turano, Murugendra Vanarotti*

c-type cytochromes are ubiquitous metalloproteins, characterized by a heme cofactor covalently bound to the polypeptide chain. Their folding/unfolding pathway(s) are been intensely studied. In particular, the influence of the heme pocket conformation versus that of the remainder of the polypeptide chain is an intriguing and not yet fully understood factor. Here the equilibrium unfolding of the *Bacillus pasteurii* cytochrome c (Bpcytc), a 'minimal' 71-aminoacid cytochrome, is investigated. The reduced length of the polypeptide chain permits highlighting the role of the loop containing the axial methionine. The native form, stable in the pH range 1.0-12 (LS) is in equilibrium with two largely unfolded forms: a low-spin form dominant under denaturing conditions (i.e. [GdmCl] > 5 M) at pH higher than 4.6 (LS1), and a high-spin form dominant under denaturing conditions at pH lower than 4.6 (HS). In both forms the Met is detached, but only in the case of the LS1 it is replaced by a protein ligand. Heme iron ligation changes take place only upon significant loss of non-covalent structure. By comparing these results with those of mitochondrial cytochromes, it is concluded that the thermodynamic stability of the region around the metal cofactor is determined by the chemical nature of the residues around the axial methionine. The isoleucine 75 in the Bpcytc (I75ABpcytc), located close to the heme pocket, is been mutated to an alanine. A denaturation study of the heme pocket by UV visible spectroscopy has been performed. The denaturation curve is similar to that of wild type Bpcytc, but the denaturation occurs at 3 M [GdmCl] instead of 3.75 M. Indicating that this position is crucial in the stabilisation of the heme pocket.

## Towards the NMR structure of hPin1

*Elena Bayer, Elena Guiberman, Peter Bayer*

hPin1 is a member of the human parvulin family of peptidyl-prolyl cis/trans isomerases, which acts as a regulator of mitosis. hPin1 shows 20.8% sequence identity to its functional homologue in yeast Ess1. Depletion of hPin1 in HeLa cells and of Ess1 in yeast result in mitotic arrest1, while over expression causes G2 arrest. hPin1 is exclusively nuclear and can be co-immunoprecipitated in a macromolecular protein complex including cell cycle regulating factors and components of the splicing machinery. Ess1 was shown to interact with the C-terminal domain (CTD) of RNA-Polymerase II (PolII) and with five other proteins that are important for RNA-PolII transcription and regulation. The N-terminal domain of hPin1 interacts with a doubly phosphorylated Tyr-pSer-Pro-hr-pSer-Pro-Ser heptad repeat of the CTD of PolII. Currently two X-Ray structures are available from the hPin1. Both pin1 structures have been crystallized in complex with small peptides. The first structure was determined with an Ala-Pro dipeptide and a sulphate ion bound to the catalytical center of the PPIase domain of hPin1. The second structure was solved with a small phospho-serine oligopeptide bound to the binding interface of the WW domain. Our aim is to determine the assignment and structure of hPin1 and its complex with phospho-peptides in solution using multi-dimensional NMR experiments.

## Solution structure of the KChIP binding domain of Kv4 potassium channels

*D. Bentrop, A.R. Graber, M. Covarrubias, B. Fakler*

Voltage-gated potassium channels (Kv) of the Kv4 (Shal) gene family contribute to controlling the frequency of slow repetitive firing and back-propagation of action potentials in neurons and shape the repolarizing phase of the action potential in heart. Kv4 currents exhibit both rapid activation and inactivation and are specifically modulated by Kv channel-interacting proteins (KChIPs). The latter proteins are small EF-hand calcium binding proteins that belong to the neuronal calcium sensor (NCS)/recoverin family. It was shown that they bind specifically to the highly conserved ~40 amino acids at the very N-terminus of the Kv4 channel protein. In this study we present the solution structure of this KChIP binding domain in 42% TFE as determined by <sup>1</sup>H NMR spectroscopy with a chemically synthesized peptide. Secondary structure is limited to a short alpha-helical stretch between residues Phe11 and Ala16.

## NMR Relaxation Evidence for Tetramers of LMW Protein Tyrosine Phosphatase in Solution

*Pau Bernado, Tomas Akerud, Jose Garcia de la Torre, Mikael Akke and Miquel Pons*

Transduction of many extracellular signals involves regulation of the level of tyrosine phosphorylation of target proteins. This is the result of a balance between the competing activities of Protein Tyrosine Kinases (PTK), and Protein Tyrosine Phosphatases (PTP). Therefore, tight regulation of both PTK and PTP is essential.

Quantitative use of relaxation rate measurement to characterize intermolecular association has been hindered by the need to know the relaxation times of the individual species involved. However, recent improvements in hydrodynamic modelling and calculations have opened the way to reliable and parameter-free predictions of the relaxation rates of individual nuclei from a known three-dimensional structure.

Using R2 and R1 measurements at four different concentrations of Bovine Low Molecular Weight PTP, and the X-ray structures of the monomer and the dimer species we have detected a previously unknown tetramer. We have characterized equilibrium constants between different species and a putative tetramerization interface, provided by the local nature of relaxation rates.

The dissociation constant of the tetramer, enhanced in a crowded environment, and its structure suggest that this specie may play a role in the regulation of PTP, since tetramer is inactive, but it can be converted in the active monomeric form. This kind of regulation suggest that tetramer can be understood as a "supramolecular proenzyme".

## Productivity of cell free protein synthesis in an Escherichia coli system

*Christian Klammt, Frank Bernhard, Vladimir Shirokov and Heinz Rüterjans*

The efficiency of the protein production with an E. coli S30 cell extract in a coupled transcription-translation system was analysed using the continuous exchange cell free (CECF) approach. During incubation, the reaction mixture was permanently dialysed against a low-molecular-weight substrate solution (feeding mix) providing sufficient nucleotides and amino acids to extend the protein synthesis for up to 24 hours. In addition, inhibitory low-molecular-weight by-products are removed from the reaction mix. Transcription is directed by the addition of purified T7-RNA-polymerase and with plasmid DNA as template. The cell free expression system enables the selectively labelling of any amino acid in the synthesized protein.

The impact of the various CECF compounds on the protein production has been analysed using green fluorescent protein (GFP) as a model system. The quality of the S30 extract isolated from different bacterial strains was compared. In addition, the preparation of the S30 extract could be optimized using a modified procedure and condensing the extract to an optimal protein concentration. Key factors essential for the productivity of the CECF system have been identified. First, an exact ratio between potassium and magnesium ions was found to be crucial. Second, the general protein production considerably depends on the concentrations of the amino acids arginine, cysteine, tryptophan, methionine, aspartic acid and glutamic acid. Third, a combined energy system using acetyl phosphate and phosphoenol-pyruvate was found to be sufficient for highest yields in protein synthesis. With the established optimized CECF system, up to 5 mg of active protein have been synthesized in a 1 ml reaction and its efficiency was found to be comparable to that of commercially available cell free systems.

The versatility of CECF systems was demonstrated by the production of milligram quantities of the enzymes DFPase from *Loligo vulgaris*, xylanase from *Bacillus agaradhaerens*, the human lectin SML-1 and the bacterial transcriptional regulator protein RcsB. Besides plasmid DNA, also linear PCR fragments could be used as templates. The high level incorporation of modified amino acids into the synthesized proteins was demonstrated.

## PARABIO - The EC NMR Research Infrastructure for metallobiomolecules

*Ivano Bertini and the CERM Staff*

Nuclear magnetic resonance (NMR) is a strategic tool in the post-genomic era. Biological macromolecules necessary for life often use metal ions as cofactors. Many of these are paramagnetic (i.e. contain unpaired electrons). The EC Research Infrastructure PARABIO, established in Florence in the new scientific Campus of the University, provides a unique environment for research in the field of NMR of metal-containing molecules. The uniqueness of the infrastructure lies in the widest range of magnetic fields available, which allows a User to combine the two main NMR approaches, namely high resolution NMR and relaxometry. The infrastructure is equipped with an 800 MHz, two 700 MHz, one 600 MHz, one 500 MHz, one 400 MHz and one 200 MHz spectrometers. There are agreements to install a 900 MHz instrument within next year. A prototype  $^1\text{H}$  dedicated HP probe for the 800 MHz spectrometer developed under a RTD contract (FMGE-CT98-0107) and other specifically designed instrumentations are available to the Users. The 500 MHz spectrometer is equipped with a Cryoprobe. The 200 MHz NMR spectrometer is a wide-bore instrument and is equipped with MAS accessories. In addition to high field NMR spectrometers, PARABIO is equipped with several instruments to perform low-field NMR studies. A high resolution variable field instrument covers the 6-90 MHz field range. A Field Cycling Relaxometer, operating in the 0.01-50 MHz range and a prototype Fast Field Cycling Relaxometer developed in the frame of an RTD contract (FMGE-CT95-0002), operating in the 0.001-20 MHz range, are available. With the EC support, we are working at the development of a High Sensitivity Fast Field Cycling NMR (Contract HPRI-CT-2001-50028), that is expected to be available in two years. A parallel computer and a large number of networked UNIX and Linux workstations are available for structure determination and refinement and for data analysis in general. PARABIO offers unique research capabilities in the field of high-resolution NMR of paramagnetic metalloproteins and other biological macromolecules which are aimed at i) solution structure determination, ii) understanding of metalloprotein folding, iii) investigation of the dynamics and mobility of these systems and iv) methodological advancements exploiting the special properties of paramagnetic biomolecules (e.g. in terms of structural constraints). Moreover, it is one of the very few laboratories in the world where relaxometry and nuclear magnetic resonance dispersion (NMRD) measurements can be performed and analysed with in-house developed programs offering great opportunities also in fields of industrial interest, such as contrast agents for magnetic resonance imaging (MRI). The growing biotechnology and molecular biology section of the facility is an integral part of PARABIO and visiting scientists will also profit from the support given to them by this part of the infrastructure.

## Colicin E9 Dissecting a Bacterial Toxin

*R. Boetzel, E. S. Collins, R. James, C. Kleanthous & G. R. Moore*

Colicins, bacterial toxins produced by *E. coli* as a response to environmental stress, are three-domain proteins consisting of a killing, a receptor-binding (R) and a translocation (T) domain. Their toxicity results from either pore-forming or nuclease activity; we are mainly interested in E-type colicins with DNase activity.

However, the size of an intact colicin is 61 kDa, which severely limits accessibility by NMR. Therefore the DNase and receptor-binding domains of Colicin E9 were expressed separately, yielding 15 and 10kDa proteins, respectively, with intact functionality.

Triple resonance NMR experiments, as well as diffusion and hydrodynamic radius measurements and relaxation time analysis allowed us to access the conformation of the receptor-binding domain in solution and to compare it to the X-ray structure of the highly homologous R domain of Colicin E3.

Having established structural information about the DNase domain in previous work we decided to approach the intact colicin E9, since the full length of the translocation domain is not entirely clear. This resulted in an  $^1\text{H}, ^{15}\text{N}$  HSQC spectrum completely different from either DNase or R domain. Further analysis of the data showed that the spectrum comprised the first 82 residues of Colicin E9 which are part of a highly flexible structure that contains a key interaction region for a protein TolB which assists with passage of the colicin into a cell and is also not observed in the electron density map of colicin E3.

Here we report our findings on the receptor-binding domain and first 82 residues of the intact colicin.

## HADDOCK: A protein-protein docking approach based on biochemical or biophysical information

*Dominguez C., Boelens R. and Bonvin A.M.J.J.*

The structure determination of protein-protein complexes is a rather tedious and lengthy process, both by NMR and X-ray crystallography. Several methods based on docking to study protein complexes have also been well developed over the past few years. Most of these approaches are not driven by experimental data but based on combination of energetics and shape complementarity. Here we present an approach called HADDOCK (High Ambiguity Driven protein-protein DOCKing) that makes use of biochemical and/or biophysical interaction data such as chemical shift perturbation data resulting from NMR titration experiments or mutagenesis data. This information is introduced as Ambiguous Interaction Restraints (AIR) to drive the docking process. An AIR is defined as an ambiguous distance between all residues shown to be involved in the interaction. The accuracy of our approach is demonstrated with three molecular complexes. For two of these complexes, for which both the complex and the free protein structures have been solved, NMR titration data were available. Mutagenesis data were used in the last example. In all cases, the best structures generated by HADDOCK, i.e. the structures with the lowest intermolecular energies, were the closest to the published structure of the respective complexes (within 2.0 Å backbone RMSD).

## Interaction of Pt(II) complexes with anticancer drug bleomycin

*Ioannis Bratsos, Barbara Mouzopoulou, Athanasios Papakyriakou and Nikos Katsaros*

Bleomycins (BLMs) are a family of glycopeptide antitumor antibiotics, isolated from a fermentation broth of *Streptomyces verticillus*. A mixture of BLMs is employed clinically for the treatment of selected neoplastic diseases, such as testicular tumors and malignant lymphomas. Their therapeutic effects are believed to derive from their ability to effect the degradation of DNA in the presence of a redox-active metal ion, such as ferrous ion, and molecular oxygen. Likewise, cis-[PtCl<sub>2</sub>(NH<sub>3</sub>)<sub>2</sub>] (cisplatin) has demonstrated a remarkable chemotherapeutic potential in a number of human solid cancers. These two antitumor compounds, which exhibit synergism, are used in combination chemotherapy to treat malignant tumors.

The interaction of bleomycin with cis-[PtCl<sub>2</sub>(NH<sub>3</sub>)<sub>2</sub>] and trans-[PtCl<sub>2</sub>(NH<sub>3</sub>)<sub>2</sub>] under different conditions has been studied. The characterization of the intermediate and final compounds arising from this work has been carried out by means of a variety of spectroscopic methods, which include UV/Vis, circular dichroism (CD), 1D NMR (<sup>1</sup>H NMR, <sup>195</sup>Pt NMR) and 2D NMR (ROESY, COSY, HMQC and HMBC).

Our data indicate that a square planar complex of BLM with Pt(II) forms slowly. Four nitrogen donors of BLM including the pyrimidine nitrogen, that of the secondary amine of the  $\alpha$ -amine alanine, the nitrogen of the imidazole and that of the histidine amide are involved in the coordination square.

## Interactions of the Anti-Tuberculosis Drug Isoniazid with Horseradish Peroxidase C

*L. Banci, J. Bodiguel, K.A. Brown, B. Jamart-Grégoire, and R. Pierattelli*

Oxidation of isoniazid, a frontline prodrug used in current treatment regimes for tuberculosis, is known to be catalyzed by the Mycobacterium tuberculosis katG-encoded catalase-peroxidase and horseradish peroxidase C (HRPC). To further elucidate molecular details of peroxidase-mediated isoniazid activation, the affinity, oxidation and binding mode of isoniazid have been investigated for HRPC using a range of spectroscopic methods. Using electron paramagnetic resonance and <sup>1</sup>H NMR spectra, we demonstrate the formation of an HRPC-isoniazid adduct and have determined apparent equilibrium affinity constants. Reaction products have also been analyzed using quantitative HPLC combined with mass spectrometry. Two-dimensional NOESY experiments allowed assignment of key structural elements of the active site of HRPC which interact with the drug. Based upon NMR data, models of the HRPC-isoniazid and HRPC-cyanide-isoniazid complexes were generated and refined using energy minimization and molecular dynamics methods. These models indicate that isoniazid binds to the enzyme in a hydrophobic pocket near the heme-18 methyl group and, interestingly, shares some similarities with the observed orientation of benzhydroxamic acid in the active site of an HRPC crystal structure. Comparison of structural and functional data between HRPC and the M. tuberculosis catalase-peroxidase also suggest that these enzymes share common features responsible for isoniazid binding and turnover.

## Dynamic Properties of the FALS mutant G93A SOD1 as Detected by NMR spectroscopy

*Francesca Cantini<sup>1</sup>, Lucia Banci<sup>1</sup>, Ivano Bertini<sup>1</sup>, Eric L. Shipp<sup>2</sup>, Joan S. Valentine<sup>2</sup>*

<sup>1</sup> Magnetic Resonance Center CERM and Department of Chemistry, University of Florence, Florence, Italy

<sup>2</sup> Department of Chemistry & Biochemistry, University of California, Los Angeles, USA

Amyotrophic Lateral Sclerosis (ALS) is a progressive neurodegenerative disease that results in a gradual degradation of motor neurons in the motor cortex, brain stem, and spinal cord. A genetic link has been found in roughly 10% of all reported cases of the disease, which are collectively referred to as Familial ALS (FALS). Of these cases, approximately one in fifth have been directly attributed to autosomal dominant mutations in the gene that encodes CuZn superoxide dismutase (SOD1).

SOD1 is a 32 kDa homodimer consisting of two Cu and Zn ions per dimer, in which the reduction and oxidation of Cu mediates the disproportionation of superoxide anion to hydrogen peroxide and dioxygen. The enzyme is composed of a Greek key β-barrel motif containing an internal disulfide bond, both of which contribute to its high stability. There are a number of conserved glycine residues found in almost all of the known CuZn SOD proteins. Moreover, five mutations of the conserved glycine at position 93 have been implicated in SOD related FALS. It has been postulated that structural destabilization and/or an increase in mobility of SOD1 mutants may play a role in the pathology of amyotrophic lateral sclerosis. In the present study, the dynamic properties of the most prevalent of the G93X FALS mutants, G93A SOD1, are investigated by nuclear magnetic resonance spectroscopy. This is the first study of the dynamic properties of a SOD1 related FALS mutant in which variations in mobility are characterized in distinct residues and concise areas of the protein.

## Effects Of Ligand Binding On The Stability And The Structural Cooperativity Of A SH3 Domain

*Casares, S., Sadqi, M., Martinez, J.C., Lopez-Mayorga, O., Van Nuland, N. And Conejero-Lara, F.*

Proline-rich peptides bind with moderate affinity to SH3 domains. The peptide APSYSPPPP (p41) binds to the Abl-SH3 domain with high affinity ( $K_d \sim 1.5 \mu\text{M}$ ) but only with moderate affinity ( $K_d \sim 83 \mu\text{M}$ ) to Spc-SH3. We have designed a R21A mutant of Spc-SH3 with an increased affinity for p41 ( $K_d \sim 40 \mu\text{M}$ ) as measured by fluorescence titration experiments. The thermodynamics of the binding of the WT domain and the R21A mutant has been studied by Isothermal Titration Calorimetry (ITC), which indicates a similar enthalpic and entropic contributions to the binding process. However the increase in affinity by the mutation has a majoritary enthalpic character indicating an optimization of interactions in the complex.

Titration of the R21A mutant with p41 has been followed by high-resolution 2D-NMR. The effect of ligand binding on the chemical shifts of the amide and alpha protons indicates that protein-ligand interactions are not confined to the binding site but are transmitted through the domain structure, mainly to the n-src and RT-loops, the most flexible regions of the domain. NMR-detected amide hydrogen exchange measurements have been performed for the R21A mutant in the free and bound states. The results provide a very interesting picture of how the interactions established in the binding site are cooperatively transmitted through the domain structure thereby stabilising it.

## Structural Genomics of Proteins Involved in Copper Homeostasis

*Ivano Bertini<sup>1</sup>, Lucia Banci<sup>1</sup>, Fabio Arnesano<sup>1</sup>, Erica Balatri<sup>1</sup>, Francesca Cantini<sup>1</sup>, Simone Ciofi-Baffoni<sup>1</sup>, Rebecca Del Conte<sup>1</sup>, Mariapina D'Onofrio<sup>1</sup>, Leonardo Gonnelli<sup>1</sup>, Stefano Mangani<sup>2</sup>, Frutos Marhuenda-Egea<sup>1</sup>, Antonio Rosato<sup>1</sup>, Francisco J. Ruiz-Dueñas<sup>1</sup>, Andrew R. Thompson<sup>1</sup>*

<sup>1</sup> Magnetic Resonance Center, University of Florence, Via Luigi Sacconi 6, 50019, Sesto Fiorentino, Italy.

<sup>2</sup> Department of Chemistry, University of Siena, Siena, Italy.

Genome sequencing projects have provided a wealth of data, and most notably the primary sequences of all the proteins that a given organism can produce. This information must match with our knowledge that number of metal ions are essential for the life. Three-dimensional structural information is necessary to unravel at atomic level the mechanisms by which a protein carries out its function, and can often be very useful to predict at least gross functional features even in the absence of biochemical data. NMR spectroscopy represents a unique tool to obtain structural and dynamics information in solution and experiments are continuously developed and improved to make NMR characterization of larger and larger molecules possible and to derive new different classes of constraints. In metalloproteins, in addition to determine the structure of the protein frame, the location of the metal ion(s) and the nature of the ligands need to be defined.

We, at CERM of the University of Florence, are developing a structural genomic program, in which, in order to enhance the functional insights provided by genome-scale structural determination, our research is prioritized to target specific processes of the cell, i.e. those responsible for controlling metal homeostasis. Results obtained on the proteins involved in the homeostasis of copper are presented. The solution structures of nine proteins have been solved in the copper-bound and/or copper-free forms: Atx1<sup>1</sup>, Ccc2a<sup>2</sup> and Cu7 metallothionein<sup>3</sup> from *Saccharomyces cerevisiae*, CopAb<sup>4</sup>, CopZ<sup>5</sup> and Sco1 from *Bacillus subtilis*, CopC<sup>6</sup> from *Pseudomonas syringae*, CutA1 and ZntA<sup>7</sup> from *Escherichia coli*. The copper coordination of these proteins has been also characterized through EXAFS technique<sup>8</sup>. With the aim of understanding the mechanism of copper trafficking in these organisms, the interactions of the copper transport proteins with their protein partners have been investigated through NMR measurements for Atx1:Ccc2a<sup>9</sup> and CopZ:CopAb<sup>10</sup> adducts. An overview of their relevance to the understanding of molecular function and cellular processes is also given.

### References

- Arnesano, F., Banci, L., Bertini, I., Huffman, D. L., O'Halloran, T. V. (2001), *Biochemistry* 40, 1528-1539.
- Banci, L., Bertini, I., Ciofi-Baffoni, S., Huffman, D. L., O'Halloran, T. V. (2001), *J.Biol.Chem.* 276, 8415-8426.
- Bertini, I., Hartmann, H. J., Klein, T., Liu, G., Luchinat, C., Weser, U. (2000), *Eur.J.Biochem.* 267, 1008-1018.
- Banci, L., Bertini, I., Ciofi-Baffoni, S., D'Onofrio, M., Gonnelli, L., Marhuenda-Egea, F. C., Ruiz-Dueñas, F. J. (2002), *J Mol Biol* 317, 415-429.
- Banci, L., Bertini, I., Del Conte, R., Markey, J., Ruiz-Dueñas, F. J. (2001), *Biochemistry* 40, 15660-15668.
- Arnesano F., Banci L., Bertini I., Thompson A. Solution structure of CopC: a cupredoxin-like protein involved in copper homeostasis. *Structure* 2002; In Press.
- Banci L., Bertini I., Ciofi-Baffoni S., Finney L.A., Outten C.E., *J.Mol.Biol.* 2002; In Press.
- Banci L., Bertini I., Del Conte R., Mangani S., Meyer-Klaucke W. X-ray absorption spectroscopy study of CopZ, a copper chaperone in *Bacillus subtilis*; submitted.
- Arnesano, F., Banci, L., Bertini, I., Cantini, F., Ciofi-Baffoni, S., Huffman, D. L., O'Halloran, T. V. (2001), *J.Biol.Chem.* 276, 41365-41376.
- Banci L., Bertini I., Ciofi-Baffoni S., Del Conte R., Gonnelli L. Hints to understand copper trafficking in bacteria: interaction between the copper transport protein CopZ and the N-terminal domain of the copper ATPase CopA from *Bacillus subtilis*; submitted.

## Effects of altering disulphide bridging on the hydrophobic clusters of non-native lysozyme

*Emily Collins, Julia Wirmer, Shin-ichi Segawa, Kenichi Hirai, Harald Schwalbe*

The characterization of non-native proteins is important, since non-native proteins not only encode the folding pathway but play an important role in cellular regulation processes and at the onset of diseases. Residual structure was detected in several proteins even under strong denaturing conditions [1,2]. Recently we have shown by relaxation measurements that hydrophobic clusters in non-native wt lysozyme are stabilized by long-range interactions: a single point mutation that replaced Trp62 with Gly disrupts all clusters.

Here we will present the effects on the relaxation rates of lysozyme when two of the four disulphide bridges (Cys64-Cys80 and Cys76-Cys94) are removed.

### References

- [1] 'Long-Range Interactions Within a Nonnative Protein' J. Klein-Seetharaman, M. Oikawa, S.B. Grimshaw, J. Wirmer, E. Duchardt, T. Ueda, T. Imoto, L.J. Smith, C.M. Dobson, and H. Schwalbe *Science* 295, 1719-1722 (2002).  
 [2] 'Persistence of Native-Like Topology in a Denatured Protein in 8 M Urea' D. Shortle and M.S. Ackerman *Science* 293, 487-489 (2001)

## Study Of The Unfolding And Oligomerization Of A SH3 Domain By Pulsed-Field Gradient NMR Diffusion Measurements.

*Casares, S., Sadqi M., Lopez-Mayorga O., Van Nuland N.A.J. And Conejero-Lara F.*

The thermal unfolding of the SH3 domain from alpha-spectrin has been previously studied at pH 3 and a range of sample concentrations from 0.03 mM to 5 mM, using differential scanning calorimetry, circular dichroism, NMR and amide hydrogen exchange. At sample concentrations higher than ca. 0.5 mM and temperatures between 40 and 70 °C, the data indicate a significant population of partially folded oligomers in equilibrium with the monomeric folded and unfolded states. Chemical cross-linking has confirmed the presence of oligomers under these conditions (from dimers to high-order oligomers depending of concentration). The hydrodynamic radius (Rh) of the different species in the unfolding equilibrium has been studied by pulsed-field gradient NMR diffusion measurements. Using the decay with the gradient strength of native NMR signals, the Rh of the native protein has been unequivocally determined. While at 20 °C the native protein has a Rh of 16.5 Å, at 50 °C its Rh decreases to 12.8 Å, a value equivalent to the radius of gyration expected for this size of molecule. At 50 °C the analysis of the decay of the whole area of the aromatic and the methyl regions of the spectra needs to assume a minimum of two species of different Rh: The native state with Rh = 12.8 Å, and a "non-native state" with Rh = 19.6 Å. Their relative populations depend strongly of the protein concentration, in good agreement with the thermal unfolding experiments. The non-native Trp-indole signal at ca. 10 ppm gives a Rh of 21.3 Å under these conditions, and equals the Rh of the unfolded chain determined under highly denaturing conditions (21.5 Å). It appears that the unfolded monomeric chain and the majoritary oligomeric species (probably dimers) cannot be easily discriminated by the NMR diffusion technique because either they have a similar Rh or they are in fast chemical exchange. Nevertheless, the dependence with protein concentration of the relative contribution of native and non-native species to the amplitude of the decays clearly confirms the presence of the oligomerization equilibrium.

## Elemental Quantitation of Natural Organic Matter by CPMAS $^{13}\text{C}$ NMR Spectroscopy

*P. Conte, A. Piccolo, B. van Lagen, P. Buurman and M. A. Hemminga*

Cross-polarized magic-angle-spinning NMR (CPMAS-NMR) techniques are assumed to be only semi-quantitative in the assessment of carbon distribution in humic substances or natural organic matter, due to a number of interferences such as spinning side bands (SSB) in spectra, paramagnetic species in samples, and low or remote protonation of aromatic carbons. Fast rotor spin rates or direct polarization NMR techniques are normally applied to improve quantitative signal detectability. Variable contact time pulse sequences were used here to obtain CPMAS-NMR spectra of organic compounds of known structure and different humic substances. Integration of spectral areas, previously subtracted of SSB, and relative stoichiometric factors were used for mathematical elaboration to calculate the elemental content in samples. These values did not significantly differ from those obtained by direct determination of elemental content with quantitative elemental analysis. Our results showed that the carbon observed CPMAS-NMR provides a quantitative representation of the whole carbon content in humic substances.

## Zinc-Binding Properties and Fold of ACE Active Sites Studied Through $^1\text{H}$ NMR & Chemical Shift Perturbation Mapping

*Athanassios Galanis, Georgios A. Spyroulias, Roberta Pierattelli, Andreas Tzakos, Ioannis Gerotheranassis, Anastassios Troganis, George Pairas, Evy Manessi-Zoupa, Paul Cordopatis*

Angiotensin Converting Enzyme (ACE) is a zinc metallopeptidase with unknown three-dimensional structure possessing an important role in the regulation of the blood pressure due to its action in the frame of the Renin-Angiotensin System. Efforts for the specific inhibition of the catalytic function of this enzyme have been made on the basis of the X-ray structures of other enzymes with analogous efficacy in the hydrolytic cleavage of peptide substrates' terminal fragments. Angiotensin Converting Enzymes bears the sequence and topology characteristics of the well-known gluzincins, a sub-family of zincins metallopeptidases and these similarities are exploited in order to reveal common structural elements among these enzymes. The synthetic peptides bear 36 amino acids which represent the primary sequence of the two ACE catalytic sites found towards enzyme's N- and C- terminus; the peptides are termed as ACEN[His361-Ala396] and ACEC[His959-994], respectively. Their zinc-binding properties have been monitored in solution through high-resolution  $^1\text{H}$  NMR. The obtained data are analysed in terms of chemical shift differences; the results indicate zinc binding to the HEMGH and EAIGD characteristic motifs and suggest the possible coordination modes of zinc in the native enzyme. According to analysis of sequential NOE,  $^3J$  coupling constants, chemical shift difference and preliminary structural calculations reveals a zinc-binding fold with features identified also for other gluzincins with known 3D structures (such as Thermolysin, Neurolysin, etc.). These features are basically the two  $\alpha$ -helical fragments at the two termini of the peptides where the three amino acid residues, coordinated to zinc metal, are found indicating a «two active helices site» for the catalytic center of ACE. Elucidation of the structural properties of these peptides could provide valuable information towards the design and preparation of new potent ACE inhibitors.

## Superoxide dismutase: structure, mobility and function

Michael Assfalg, Lucia Banci, Ivano Bertini, Francesca Cantini, Fiorenza Cramaro, Rebecca Del Conte, Mariapina D'Onofrio, Paola Turano, Paul Vasos, Maria Silvia Viezzoli

The structures of wild type dimeric human SOD and of two mutants (E133QM2SOD<sup>1</sup> and M4SOD<sup>2</sup>) which are in a monomeric state, were determined in solution through NMR spectroscopy. Furthermore, the dynamical properties of these systems were analysed on the ns-ps and ms-ms time ranges<sup>3</sup>.

The structures and mobility were compared with the goal of correlating the quaternary structure with the enzymatic efficiency of these species.

Meaningful differences were observed between the wild type dimeric protein and the monomeric species both in structure and in mobility at the subunit-subunit interface as well as in the electrostatic active channel. To understand the uptake of the metal ions and its possible correlation with the FALS disease the determination of the solution structures of apo-<sup>4</sup> and single- metallated (Cu depleted) SOD<sup>5</sup> have been studied.

The single- metallated (Cu depleted) SOD structure constitutes a model for the SOD state which interacts with the copper chaperone CCS, as it represents SOD state before copper uptake. Structural and dynamical studies on this protein have been carried out and data compared with those of the wild type protein.

The apo-protein has a well defined tertiary structure; however,  $\beta$ 4,  $\beta$ 5,  $\beta$ 7 and  $\beta$ 8 strands move away from the other ones of the  $\beta$  barrel and form an open clam with respect to a close conformation in the holoprotein. The structural and mobility data, if compared to those of the copper-depleted and holo-proteins, point out the role of each metal ion in the protein folding, leading to the final tertiary structure of the holoprotein and provide hints for the mechanisms of metal delivery by metal chaperones.

The role of the metal ions in the protein stability has been further investigated through an NMR study of the unfolding of monomeric SOD induced by chemical denaturants.

### References:

- (1) Banci, L., Benedetto, M., Bertini, I., Del Conte, R., Piccioli, M. & Viezzoli, M. S. (1998). *Biochemistry* 37, 11780-11791.
- (2) Banci, L., Bertini, I., Del Conte, R., Mangani, S., Viezzoli, M. S. & Fadin, R. (1999). *JBIC* 4, 795-803.
- (3) Banci, L., Bertini, I., Cramaro, F., Del Conte, R., Rosato, A. & Viezzoli, M. S. (2000). *Biochemistry* 39, 9108-9118.
- (4) Banci L, Bertini I, Cramaro F, Del Conte R, Viezzoli MS. 2003 (Submitted)
- (5) Banci, L., Bertini, I., Cantini, F., D'Onofrio, M. & Viezzoli, M. S. (2002). *Protein Sci.* 11, 2479-2492.

## Structure and functional aspects of Cu-thiolate clusters in intact and truncated forms of yeast Cu-metallothionein

Claudio Luchinat<sup>1</sup>, Benedikt Dolderer<sup>3</sup>, Cristina Del Bianco<sup>1</sup>, Ivano Bertini<sup>1</sup>, Hans-Jürgen Hartmann<sup>3</sup>, Hartmut Echner<sup>2</sup>, Wolfgang Voelter<sup>2</sup>, Ulrich Weser<sup>3</sup>

<sup>1</sup>Magnetic Resonance Center, University of Florence, Sesto Fiorentino, Italy;

<sup>2</sup>Physikalische Biochemie, Eberhard-Karls-Universität Tübingen, Germany;

<sup>3</sup>Anorganische Biochemie, Eberhard-Karls-Universität Tübingen, Germany.

Two fragments of yeast Cu7-metallothionein containing all of the ten copper-coordinating cysteine residues were prepared by solid phase peptide synthesis. In both truncated peptides thirteen C-terminal amino acid residues were omitted. Additionally, residues 1-4 were absent in the shorter peptide form (peptide 5 - 40). The N-terminus of the other species was elongated by one tyrosine residue (peptide 1 - 40) hoping that possible hydrophobic interactions of the aromatic ring would facilitate crystallization of the peptide. Shortening of the polypeptide matrices did essentially not affect the characteristic spectroscopic features of the wild type protein including UV electronic absorption, circular dichroism and luminescence emission. It should be emphasized that all heptanuclear Cu-thiolate clusters were structurally identical regardless of the polypeptide backbone. In the 2D <sup>1</sup>H-<sup>1</sup>H-NOESY spectra of all three species, the observed spin patterns were very similar. The NMR data was used to run structure calculations for the longer fragment and the wild type protein resulting in identical structures. All copper-coordinating cysteines were found in the same positions in either protein. Although these results were suggestive of identical Cu-thiolate clusters in the three species, some differences in terms of reactivity were observed for the fragments. Under aerobic conditions peptide 5 - 40 lost its luminescence completely within 24 h, whereas for the wild type protein and peptide-1 - 40 the luminescence half lives were determined at 48 h and 24 h, respectively. This behaviour was consistent with different oxygen accessibility of the Cu-thiolate clusters observed by different luminescence quenching. Incubation of the three species with a hundredfold excess of the Cu(I)-chelator bathocuproine disulfonic acid revealed that the wild type protein lost its copper more readily than the two fragments. This might be attributed to the cysteines 49 and 50, that are missing in the truncated forms. These two residues might compete for the cluster-bound copper and therefore facilitate the copper release.

## Relaxometric Investigation of Polysaccharide-Protein Conjugate Vaccines

*I. Bertini, M. Fragai, C. Luchinat*

A relaxometric investigation of a mutant of Diphtheria toxin and of its conjugates with capsular polysaccharides of different groups of *Neisseria Meningitidis* was performed. The presence of polysaccharides chains alters dramatically the hydrodynamic and relaxometric properties of the protein. The effects of the degree of conjugation and of the length of polysaccharides moieties on the water solvent relaxation properties have been analyzed with a model-free approach. The values of the average correlation times as a function of conjugate concentration permit a characterization of the conjugates in terms of an interplay between aggregation and internal mobility.

## NMR study of structural properties of polyubiquitin chains in solution

*Ranjani Varadan, Olivier Walker, Cecile Pickart, and David Fushman*

Polyubiquitin chain structure modulates Ub-mediated signaling. Therefore, knowledge of the physiological conformations of chain signals should provide insights into specific recognition. We characterized the solution conformations of K48-linked Ub<sub>2</sub> and Ub<sub>4</sub> using a combination of chemical shift mapping, <sup>15</sup>N relaxation anisotropy, and residual dipolar coupling measurements. Our NMR data indicate a switch in the conformation of Ub<sub>2</sub>, from open to closed, with increasing pH. The closed conformation features a well-defined interface that is related to, but distinguishable from, that observed in the Ub<sub>2</sub> crystal structure. This interface is dynamic in solution, such that important hydrophobic residues (L8, I44, V70) that are sequestered at the interface in the closed conformation may be accessible for direct interactions with recognition factors. Our results suggest that the distal two units of Ub<sub>4</sub>, which is the minimum signal for efficient proteasomal degradation, adopt the closed Ub<sub>2</sub> conformation.

## Lanthanide Ions As NMR Probes Of Peptides Interacting With Receptor Sequences

*Elena Gaggelli, Nicola D'Amelio, Nicola Gaggelli, Elena Molteni, Daniela Valensin, Gianni Valensin*

Lanthanide ions may be used as nmr probes of the interaction between bioactive peptides and peptide sequences obtained from the receptor target. The shifts and relaxation rate enhancements induced by lanthanides on selected proton and/or carbon resonances of the bioactive peptide can be used to track the role of the same residues in the interaction with synthetic peptide sequences taken from the receptor. As an example, the role played by Ce(III) ions on delineating the interaction of Ang II with a 21 aminoacid sequence taken from the C-terminal part of the angiotensin receptor will be illustrated

## Interactions of the $\Lambda$ , and $\Delta$ -[Ru(bpy)<sub>2</sub>(m-GHK)]Cl<sub>2</sub> enantiomers with the oligonucleotide d(CGCGAATTCGCG)<sub>2</sub>, where m-GHK=4-methyl-4'-glycyl-histidyl-lysine-2,2'-bipyridine

*Alexandra Myari<sup>1</sup>, Achilleas Garoufis<sup>1</sup> and Nick Hadjiliadis<sup>1</sup>*

<sup>1</sup>University of Ioannina, Department of Chemistry, Ioannina 45110, Greece E-mail: nhadjis@cc.uoi.gr

The intercalation of metal complexes into DNA and direct binding of them with DNA base pairs has been a major field of research in recent years. The ruthenium(II) polypyridyl complexes are an important class of metallointercalators; however their DNA binding is not as yet well understood. Initial studies of the parent ruthenium(II) polypyridyl, [Ru(phen)<sub>3</sub>]<sup>2+</sup>, suggested the existence of two modes of binding, a minor groove surface bound interaction, and a major groove intercalated form<sup>1</sup>. Furthermore, it was proposed that the  $\Lambda$  - and  $\Delta$  - enantiomers of Ru(II) complexes bind to DNA in a different manner<sup>2</sup>. However, sequence selectivity upon binding to the DNA macromolecule still remains under question.

In an attempt to investigate the sequence selectivity upon binding to DNA of the Ru(II) bipyridyl complexes and facilitate the transporting of an antitumor complex through membranes, the tripeptide Gly-His-Lys was attached to one bipyridyl molecule. The interactions of  $\Lambda$ ,  $\Delta$ -[Ru(bpy)<sub>2</sub>(m-GHL)]Cl<sub>2</sub> enantiomers with the oligonucleotide d(CGCGAATTCGCG) have been studied using 1D and 2D <sup>1</sup>H NMR and CD spectroscopy. The results will be discussed and the possible binding modes of the two enantiomers will be deduced.

### References

1. Rehmman, J. P., Barton, J. K. *Biochemistry* 1990, 29, 1701; *Ibid.* P. 1709
2. Garoufis, A., Liu, J. G., Ji, L. N., Hadjiliadis, N. *J. Inorg. Biochem.*, submitted for publication

## New Algorithms for Advanced NMR Processing

*Ulrich Günther, Heinz Rüterjans*

Although NMR processing seemed satisfactory since the introduction of the fast Fourier transform recent development shows substantial potential for novel numerical algorithms. One of the main issues is noise reduction, an important step for automatic data analysis. Wavelet transforms offer new possibilities for several steps of NMR processing, including denoising of NMR spectra, efficient solvent suppression and improved analysis of series of spectra obtained in drug screening. Denoising was combined with efficient peak picking to provide highly accurate NOESY peak lists for automatic structure calculation [1,3]. Solvent suppression was achieved using a new wavelet-based algorithm (WAVEWAT) [2]. Clustering of similar spectra was improved by combining wavelet transforms and principal component analysis.

### References

1. U. Günther, C. Ludwig, H. Rüterjans. NMRLAB - Advanced NMR Processing in MATLAB. *J. Magn. Reson.* 145, 201-208 (2000)
2. U. Günther, C. Ludwig, H. Rüterjans. WAVEWAT - Improved Solvent Suppression in NMR Spectra Employing Wavelet Transforms. *J. Magn. Reson.* 156, 19-25 (2002)
3. U. Günther, C. Ludwig, H. Rüterjans. Improved Automatic Structure Calculation Using Wavelet Denoised Spectra. Submitted.

## NMR studies on conformation of heparin oligosaccharides bound to proteins

*M. Guerrini, M. Hricovini, A. Bisio, G. Torri, B. Casu*

Heparin is an acidic polysaccharide made up of alternating uronic acids (alpha-L-Iduronic acid and beta-D-glucuronic acid) and alpha-D-glucosamine, with different degrees and patterns of sulfation. Most of the biological properties of heparin are associated with interaction with proteins through specific binding sequences. The knowledge of structure and conformation in the protein binding site of these sequences is a requirement to fully understand the natural functions of heparin and to develop new drugs in important therapeutic areas.

In the present work different NMR parameters such as NOEs and transferred NOEs, proton and carbon chemical shifts and coupling constants were used to study the conformation of heparin oligosaccharides in both free and bound state. Two dimensional NOESY experiments were interpreted using the Complete Relaxation and Conformational Exchange Matrix analysis (CORCEMA). The theoretical NOEs were based on the geometry of the oligosaccharide found in a Monte Carlo conformational search and the three-dimensional structures of the oligosaccharides in bound and free state were derived.

The analysis of the three-dimensional structure of oligosaccharides bound to antithrombin, acidic fibroblast growth factor and basic fibroblast growth factor in solution are presented.

### References

- 1 Hricovini, M. Guerrini, A. Bisio, G. Torri, M. Petitou and B. Casu *Biochem J.* 2001, 359, 265272
- 2 M. Guerrini, et al. *BBRC* 2002, 292, 222-230.

## Resolving the 3D-Structure of the Protein Amoebapore A

*Oliver Hecht, Heike Bruhn, Matthias Leippe, Joachim Groetzinger*

The pathogenic protozoon *Entamoeba histolytica* settles in the colonic lumen of infected men. In the majority of cases it lives there in a commensal manner using bacteria as a major nutrient source. To kill the phagocytosed bacterias it uses an array of bacteriolytic factors, among other things, there are pore-forming peptides called amoebapores.

Amoebapore A is one of the three isoforms of amoebapores found in *Entamoeba histolytica*. Prior investigations revealed this protein as a member of the saposin-like proteins (SAPLIPs), characterized by amphiphatic motifs with conserved locations of six cysteine residues. Other members of the SAPLIP-family, namely granulysin and NK-lysin, which are effector proteins of human and porcine lymphocytes have been compared with the amoebapores. Despite of their evolutionary distance all these polypeptides exhibit a considerable sequence similarity and furthermore they all show antibacterial activity. Whether there are also differences between these molecules with respect to charge distribution and core packing it would be an interesting question whether these proteins have developed from a common ancestor or if the similarities are a product of convergent evolution. The three-dimensional structure of 77-residue polypeptide Amoebapore A from *Entamoeba histolytica* is now in process to be resolved by NMR.

## Side chain dynamics monitored by $^{13}\text{C}$ - $^{13}\text{C}$ cross relaxation

*Klaartje Houben and Rolf Boelens*

It is widely recognized that internal motions play an important role in the biological function of proteins. NMR relaxation studies allow the characterization of these motions at atomic detail. In particular,  $^{15}\text{N}$  relaxation rates are used to determine local mobility of the backbone. However studies of side chain dynamics are still very few and mainly based on deuterium relaxation studies. It has been shown by both Zeng et al. and Cordier et al. that measurements of  $^{13}\text{C}$ - $^{13}\text{C}$  cross-relaxation rates are indicative of the motion of the Ca-CO vector. These measurements allow a further definition of the backbone mobility. Here we propose to measure cross relaxation rates between all carbon nuclei in the side chain.

Cross-relaxation rates can be determined either by measuring the steady-state NOE in presence of a saturating field or by measuring the transient NOE by inversion of one of the spins. We chose to measure the transient NOE using the 3D (H)CCH-NOESY experiment. By use of different NOE mixing times cross-relaxation rates  $\sigma$  can be determined by the initial slope of the build-up curve. In the case of homonuclear cross-relaxation  $\sigma$  is dominated by  $J(0)$ . In the Lipari-Szabo model  $J(0)$  is proportional to  $\tau_C$  times the order parameter  $S^2$ . Thus low absolute values of  $\sigma$  are an indication of fast local motions in the side chain.

The experiment was performed on  $^{15}\text{N}$ - $^{13}\text{C}$  labeled subtilisin PB92 in  $\text{D}_2\text{O}$ . Cross-relaxation rates could be measured for the majority of  $^{13}\text{C}$ - $^{13}\text{C}$  vectors in the side chains of all residues.

## Organic structure of coals of varying rank as determined by $^{13}\text{C}$ CP/MAS NMR spectroscopy

*A. Iordanidis, A. de Jager, A. Georgakopoulos, C. Dijkema, B. van Lagen*

Four coal samples, collected from Greek and Bulgarian coal fields, were studied using  $^{13}\text{C}$  CP/MAS NMR spectroscopy. The samples were chosen as representatives of various coal ranks (peat, xylite, lignite and sub-bituminous respectively). The investigation focused on the differentiation in their organic structure, as well as the percentage contribution of the major functional groups in each sample. The quantitative reliability of the CP/MAS technique was testified in a previous study, indicating the optimum values for contact and delay times. For quantification, the  $^{13}\text{C}$  NMR spectra were investigated using the integration routine of the spectrometer. The chemical shift regions 0-45, 45-100, 100-165, 165-190 and 190-220 ppm were assigned to aliphatic-C, carbohydrates, aromatic-C, carboxylic-C and carbonylic-C species respectively. The greatest amounts of aromatic structures are observed in the sub-bituminous coal, whilst lignite shows the greatest amounts of aliphatic groups. Increased contents of carboxylic species and carbohydrates are observed in the peat sample, while xylite reveals high contents of carbohydrates. Special consideration should be taken when calculating the aromaticity fraction (fa), due to the discrepancies caused by the formulae used.

## Structure and Dynamics of the two domain protein Pin1

*Doris Jacobs, Krishna Saxena, Martin Vogtherr, Klaus Fiebig*

The peptidyl-prolyl cis-trans isomerase (PPIase) Pin1 (18.4 kDa) consists of a N-terminal WW domain (Pin1\_WW) which is important in substrate targeting, and a C-terminal catalytic domain (Pin1\_Cat) which is structurally homologous to the FKBP-class of PPIases.

Pin1 selectively isomerizes peptides containing phospho-Ser/Thr-Pro sequence motifs. These peptides interact not only with Pin1\_Cat but can also bind to Pin1\_WW. Selectivity is achieved by two specific phosphate binding sites located next to the active site of Pin1\_Cat and within the peptide binding epitope of Pin1\_WW. Two X-ray studies have characterized these Pin1-peptide interactions previously: the structure of a dipeptide bound to the presumed active site of Pin1 (Ranganathan et al.), and the structure of Pin1 complexed to a doubly phosphorylated peptide peptide (Verdecia et al.). Also, a  $^1\text{H}$  NMR study (Wintjens et al.) has compared the structure of free Pin1\_WW with Pin1\_WW in complex with the Cdc25 and the tau phospho-Thr peptides.

In this study we use NMR methods to address the impact of peptide binding on the two domain nature of Pin1. We have analyzed  $^{15}\text{N}$  spin relaxation data in order to compare the domain flexibility of free and of peptide bound Pin1.  $^{15}\text{N}$  NOE data clearly show two well structured domains separated by a 20 amino acids long flexible linker. Without peptide bound to Pin1, the relaxation data of the two domains must be fit separately. Thus Pin1\_WW and Pin1\_Cat tumble isotropically with average overall correlation times  $\tau_c$  of 7.7 ns and 9.7 ns, respectively. In comparison,  $\tau_c$  of Pin1\_WW alone is 4.1 ns indicating that the linker induces weak interactions between Pin1\_WW and PinCat.

The flexibility of the two domains is significantly restricted when the peptide WFYpSPR is bound to Pin1, as evidenced by the increased  $\tau_c$  of 9.5 ns for Pin1\_WW and 10.5 ns for Pin1\_Cat. Unfortunately it was only possible to 90% saturate Pin1 with the peptide. Hence extrapolating the relaxation data of Pin1\_WW to 100% saturation resulted in approximately equal  $\tau_c$ 's for both domains. Thus, the peptide-bound Pin1 tumbles isotropically as a whole molecule with a  $\tau_c$  of 10.7 ns.

To localize the interaction surface of Pin1 and the peptide we used differential chemical shift mapping employing full length Pin1 and various deletion mutants. As expected from the relaxation data the peptide not only interacts with the PinCat active site and the peptide binding site of the Pin1\_WW domain, but also is involved in interactions at the Pin1\_WW/Pin1\_Cat domain-domain interface. Hence in agreement with the relaxation data, we conclude that the peptide causes the independent Pin1\_WW and Pin\_Cat domains to interact.

### References

- Ranganathan et al. (1997) Cell, 89, 875-86.
- Verdecia et al. (2000) Nat. Struct. Biol., 7, 639-43.
- Wintjens et al. (2001) J. Biol. Chem., 276, 25150-6.

## Axial Ligand-Metal interaction in Rusticyanin: $^1\text{H}$ NMR studies on Met148 Mutants.

*Beatriz Jiménez, José-María Moratal, John F. Hall, S. Samar Hasnain, and Antonio Donaire.*

Blue Copper Proteins (BCP's) are electron transfer mononuclear copper proteins distinguished by their singular spectroscopic features and high redox potentials. The unusual spectroscopic properties of BCP's in the oxidized state, namely, an intense ligand-to-metal charge transfer band in the visible absorption spectrum, and a small  $A_{\parallel}$  hyperfine coupling constant in the EPR signal, have been attributed to the high covalence of the conserved Cu(II)-Sg(Cys) moiety. The coordination sphere of the copper ion in BCP's is completed by two histidine residues, and a weaker, axial ligand (a Met residue in most cases). The importance of this axial ligand has been extensively debated in terms of their role in modulating the properties of BCP's.

Rusticyanin, from *Thiobacillus ferrooxidans*, is the BCP with the highest redox potential. It also has a high stability in a wide range of pH's. We are studying some copper(II) Rusticyanin mutants on the axial methionine (Met148) through  $^1\text{H}$  NMR at a magnetic field of 800 MHz. Here, we present the assignment of the hyperfine shifts of the  $^1\text{H}$  NMR spectra of five Cu(II)Rc Met148 mutants. The differences in the electronic structure of the metal ion due to the variation of the axial ligand are also discussed.

## NMR studies on protein dynamics in the bacterial DNA-helicase inhibitor KID

*Monique B. Kamphuis, Ramón Díaz-Orejas, and Rolf Boelens*

KID is a small plasmid-encoded protein that can inhibit the E.coli replication by forming an inactive complex with DnaB helicase [1]. The toxin KID itself is inactivated by complex formation with the antitoxin KIS. The interactions of KID with KIS and bacterial helicases can be used as a model system for the development of new antibiotics targeted at bacterial helicases. Therefore we will determine the structure and dynamics of the 12 kD dimeric protein KID and define the interaction surface of the toxin with helicases, using NMR spectroscopy. Because a solution structure of KID is not available yet, we started with the complete NMR assignment of  $^{13}\text{C}/^{15}\text{N}$ -labeled KID. This allowed us to predict the secondary structure of KID and compare it to that of the DNA gyrase inhibitor CcdB for which an X-ray structure exists [2]. Because of a high structural similarity between the two proteins, the CcdB structure will serve as a model for the 3D KID structure, which is still in progress. The structure of KID includes several loop regions. Microbiological studies suggest that the dorsal loop (residues 12 to 22) is responsible for the interaction of the toxin with DnaB helicase, while the head/tail loop (residues 47 to 58 and 63 to 70) forms the interaction site with KIS. To investigate the dynamic properties of KID and in particular the flexibility of the mentioned loop regions, we performed  $^{15}\text{N}$   $T_1$ ,  $T_2$  and  $^{15}\text{N}$  heteronuclear NOE measurements. These NMR relaxation experiments clearly show that the suggested interaction site (head/tail loop) of the toxin KID with the antitoxin KIS contains a highly flexible loop comprising residues 48 to 55, while the remainder of the backbone of the KID protein is remarkably rigid.

### References

- [1] Ruiz-Echevarría, M.J.; Giménez-Gallego, G.; Sabariego-Jareño, R.; Díaz-Orejas, R. J. Mol. Biol. 1995, 247, 568-577.
- [2] Loris, R.; Dao-Thi, M.-H.; Bahassi, E.M.; Melderen, L. van; Poortmans, F.; Liddington, R.; Couturier, M.; Wyns, L. J. Mol. Biol. 1999, 285, 1667-1677.

## Interactions Of Insulin-Mimetic VO(IV) Complexes With Serum Proteins Albumin And Transferrin

*Tamas Kiss, Dominik Hollender, Kirill Nerinovski, Claudio Luchinat*

Since the discovery of the insulin-like effects of vanadium complexes [1], extensive research works have been made not only to prepare and test newer and newer complexes, but also to monitor their possible transformations and to determine their actual chemical forms during their transport in the blood and in the target muscle or fat cells where they exert the physiological actions [2].

In our earlier works by studying the interactions of several vanadium complexes with the low molecular mass (l.m.m.) components of blood serum (such as citrate, phosphate, lactate and oxalate) we could describe the speciation of VO(IV) in the l.m.m. fraction of serum. In this paper we report our recent results obtained for the interactions of these insulin mimic VO(IV) complexes with the high molecular mass (h.m.m.) fraction serum proteins. Detailed room temperature and frozen solution EPR measurements, NMRD relaxation studies and the application of separation techniques proved that albumin cannot compete with transferrin in binding VO(IV) even at serum conditions when albumin is a 20-fold excess to transferrin. Ligand competition reactions between the proteins and some of the VO(IV) carrier ligands made us possible to determine/estimate conditional stability constants for binding VO(IV) to apotransferrin (apo-TF) and albumin (HAS) at pH 7.4, which are  $\log K = 13.2 \pm 0.8$  for apotransferrin and  $\log K < 10$  for albumin. These results are in contradiction with an earlier literature report [3] suggesting a value of 6 for the ratio  $K(\text{VO-apoTF})/K(\text{VO-HSA})$ .

### References

- [1] Y. Shechter, S.D.J. Karlish, Nature, 1980, 284, 556-558.
- [2] D. Rehder, J. Costa Pessoa, C.F.G.C. Geraldes, M.M.C.A. Castro, T. Kabanos, T. Kiss, B. Meier, G. Micera, L. Pettersson, M. Rangel, A. Salifoglou, I. Turel, D. Wang, J. Biol. Inorg. Chem., 2002, 7, 384-396.
- [3] N.D. Chasteen, J.K. Grady, C.E. Holloway, Inorg. Chem., 1986, 25, 2547-2560.

## Use of long distance NOEs in a fully deuterated protein; an approach for rapid protein fold determination

*L.M.I. Koharudin, A.M.M. Bonvin, R. Kaptein, and R. Boelens*

Long distance NOEs between amide protons in a fully deuterated protein that are beyond the limited distances currently observed have been measured with the help of high sensitivity of modern NMR instrument. The measurement of long distance NOEs were enabled by applying very long mixing time and this is possible thank to the very long T1 relaxation time of the amide protons. The longest distance that could be observed is up to 8.0 Å and this information was used for structure determination.

Facilitating NOE information only from the backbone amide protons resulted in an ensemble structure with RMSD to the average of 1.2Å and 2.4Å for all backbone and heavy atoms respectively. No mirror image problem was observed on the calculated structures upon use of these very long distance NOEs. Addition of side chain increased the precision of the ensemble structure. The structures obtained by this methodology were comparable to the published crystal structure. NOE completeness analysis was carried out and showed that the cumulative completeness is still more than 80% for an 8.0Å cut-off distance. Using completely deuterated protein, automated analysis of the triple resonance spectra for backbone atom chemical shift assignments may also become possible.

## NMR characterization of a mutant lac headpiece with altered operator specificity

*R. Kopke Salinas, C. Kalodimos, G. Folkers, R. Boelens and R. Kaptein*

The lac repressor controls the regulation of the expression of genes involved in the metabolism of lactose in bacteria by simultaneously binding to its natural operator O1, and to one of the auxiliary operators O2 or O3. All three lac operators are pseudo palindromic sequences, which demonstrates that the protein is able to recognize specifically different DNA sequences. It is also known that, although specific, the affinity of lac repressor for its three operators differs.

Addressing the problem of specificity of lac repressor Muller Hill and co-workers (Lehming et al., 1990; Sartorius et al., 1989) screened several mutations both on the repressor and on the DNA. It was observed that the first two residues of the repressor's recognition helix are key elements for defining specificity. By changing them for other residues it is possible to obtain mutant repressors which displays altered DNA specificity.

Tyr17 and Gln18 are the first and second residues of the recognition helix. Indeed, the structure of the lac headpiece complexed with its natural operator O1 (Kalodimos et al., 2002) showed that they make most of the specific contacts of the recognition helix with the major groove of the DNA. Lehming and co-workers (Lehming et al., 1990) showed that by changing Tyr17 and Gln18 for the same residues found in the gal repressor (Val and Ala, respectively) a mutant lac repressor that displays specificity for a gal-like operator is obtained. In an attempt to understand the role of these two residues in defining the specificity of lac repressor we designed a mutant lac headpiece containing Val and Ala at positions 17 and 18, respectively. The protein was labeled with  $^{15}\text{N}$ , and assignment of the resonances in the free form were accomplished by  $^1\text{H}$ - $^{15}\text{N}$  NOESY-HSQC and  $^1\text{H}$ - $^{15}\text{N}$  TOCSY-HSQC experiments. Titration with the gal-like operator was followed by  $^{15}\text{N}$ - $^1\text{H}$  HSQC spectra, and demonstrated that it is able to bind DNA. It is expected that the study of the specific contacts that Ala17 and Val18 make with the DNA, will help in understanding the key role that residues in these two positions play on the specificity of the lac repressor.

### References

- Lehming, N. Sartorius, J., Kisters-Woike, B., von Wilcken-Bergmann, B. and Muller-Hill, B. (1990) EMBO J. 9: 615-621.  
 Sartorius, J., Lehming, N., Kisters, B. von Wilcken-Bergmann, B. and Muller-Hill, B. (1989) EMBO J. 8: 1265-1270.  
 Kalodimos, C., Bonvin, A.M.J.J., Salinas, R.K., Wechselberger, R., Boelens, R. and Kaptein, R. (2002) EMBO J. 21: 2866-2876.

## A further investigation of the cytochrome b5 - cytochrome c complex

*Lucia Banci, Ivano Bertini, Isabella C. Felli, Ludwig Krippahl, Karel Kubicek, José J.G. Moura, Antonio Rosato*

The interaction of reduced rabbit cytochrome b5 with reduced yeast iso-1 cytochrome c has been studied through the analysis of  $^1\text{H}$ - $^{15}\text{N}$  HSQC spectra, of  $^{15}\text{N}$  longitudinal (R1) and transverse (R2) relaxation rates, and of the solvent exchange rates of protein backbone amides. For the first time, the adduct has been investigated also from the cytochrome c side. The analysis of the NMR data was flanked by docking calculations. It appears that cytochrome b5 has two negative patches capable of interacting with a single positive surface area of cytochrome c. At low protein concentrations and in equimolar mixture, two different 1:1 adducts are formed. At high concentration and/or with excess cytochrome c, a 2:1 adduct is formed. All the species are in fast exchange on the scale of differences in chemical shift. By comparison with literature data, it results that the structure of one 1:1 adduct changes with the origin or primary sequence of cytochrome b5. The present results allow an evaluation of previous models, thus settling a long term debate.

## Effect of the Hypersolute Diglycerol Phosphate on the Conformational Mobility of *D. gigas* Rubredoxin

*Lamosa, P., Turner, D.L., and Santos, H.*

The stabilisation of proteins by small compatible solutes like glycerol is known to biochemists for more than a century. However, the discovery of the unusual solutes, accumulated by hyperthermophiles (also called hypersolutes) in response to supraoptimal conditions of temperature or salinity has triggered a renovated interest in the field. The remarkable thermostabilising properties of these hypersolutes suggest their importance in extrinsic stabilisation *in vivo*.

A triple approach involving heteronuclear NMR relaxation measurements for dynamics studies, hydrogen exchange data, and the search for specific interactions was employed to characterise protein behaviour in the presence or absence of solutes. Rubredoxin from *D. gigas* was selected as a model protein and its dynamical behaviour probed in the presence of diglycerol phosphate (DGP). Hydrogen exchange data was acquired showing an additional structural stabilisation of 2.3 kJ.mol<sup>-1</sup> in the presence of DGP. This solute induces a marginal overall reduced mobility in the protein backbone with an average increase of generalised order parameters of 0.015. Using an NMR triple resonance experiment <sup>13</sup>C-<sup>1</sup>H-<sup>15</sup>N-HMQC-NOESY-HSQC no specific interaction between rubredoxin and the solute DGP was detected. The results seem to indicate that the stabilising effect is mainly due to a generalised rigidification of protein structure associated with a reduction in the mobility of large groups.

## Structure determination of the CHORD1 domain of RAR1, a signalling protein involved in disease resistance in plants

*Cécile Le Duff<sup>1</sup>, Pedro Rocha<sup>2</sup>, Rainer Wechselberger<sup>3</sup>, Ken Shirasu<sup>2</sup>, Colin Kleanthous<sup>1</sup> & Geoffrey Moore<sup>4</sup>*

<sup>1</sup>School of Biological Sciences, University of East Anglia, Norwich NR4 7TJ, UK

<sup>2</sup>The Sainsbury Laboratory, John Innes Centre, Colney Lane, Norwich NR4 7UH, UK

<sup>3</sup>Bijvoet center for Biomolecular research, Utrecht University, Padualaan 8, 3584 CH Utrecht, The Netherlands

<sup>4</sup>School of Chemical Sciences, University of East Anglia, Norwich NR4 7TJ, UK

The RAR1 gene, identified in barley, is required for resistance against a range of pathogenic powdery mildew fungi. In addition, silencing the RAR1 homolog in *C.elegans* results in a phenotype reminiscent of the well-characterised cell death mutants, *ced-3* and *ced-4* (Shirasu et al., 1999).

These observations indicate that RAR1 is an essential signalling component involved in cell death in animals and disease resistance in plants. The RAR1 gene encodes a novel protein containing three 80 residue domains named CHORD1 and CHORD2, both of which bind zinc, and the CCH domain. CHORD1 and CHORD2, although highly homologous have been shown to interact with different partners through yeast two-hybrid experiments.

A biophysical characterisation of the CHORD1 domain of RAR1 has been carried out; circular dichroism studies have shown that the secondary structure elements in CHORD1 are mainly  $\beta$ -sheets. Triple resonance NMR spectra of the overexpressed CHORD1 domain labelled with <sup>15</sup>N and <sup>13</sup>C have allowed the assignment of 75 of its 79 backbone resonances.

This poster presents the progress achieved towards the calculation of the structure of the CHORD1 domain.

## Assignment of $^1\text{H}$ , $^{13}\text{C}$ and $^{15}\text{N}$ backbone resonances of the 35-kDa protein DFPase from *Loligo vulgaris*

*Frank Löhr, Vicky Katsemi and Heinz Rüterjans*

Diisopropylfluorophosphatase (DFPase) is a monomeric 314-residue enzyme, initially isolated from the head ganglion of the squid *Loligo vulgaris*, which hydrolyzes di-isopropylfluorophosphate and a wide variety of chemical warfare agents, including sarin, soman and tabun. NMR assignments for proteins of that size are usually obtained using perdeuterated samples in order to eliminate efficient  $^1\text{H}$ ,  $^1\text{H}$  and  $^1\text{H}$ ,  $^{13}\text{C}$  dipolar spin relaxation pathways and  $^1\text{H}$ ,  $^1\text{H}$  scalar couplings. However, this requires amide protons be back exchanged after protein expression using  $\text{D}_2\text{O}$ -based bacterial growth media. While back exchange often occurs during isolation and purification of the protein in  $\text{H}_2\text{O}$ -based buffers, in the case of DFPase approximately one third of the backbone amides remain deuterated, because they are either involved in strong hydrogen bonds or deeply buried inside the protein.

To overcome this difficulty, a  $^2\text{H}$  enriched sample of recombinant DFPase was prepared by culturing *E. coli* in fully deuterated algal lysate medium in 100%  $\text{H}_2\text{O}$ , resulting in high deuterium levels in side chain positions, while all amide nitrogens are completely protonated. Incorporation of water protons during biosynthesis of amino acids depleted during bacterial growth leads to varying degrees of deuteration at Ca sites depending on amino acid types. Compared to a perdeuterated sample the higher proton density gives rise to less favourable relaxation properties, somewhat reducing sensitivity of HN-directed triple-resonance experiments. On the other hand, the presence of  $\alpha$ -protons provides independent means to obtain intraresidual and sequential connectivities within the protein backbone.

Using the  $^1\text{H}/^2\text{H}/^{13}\text{C}/^{15}\text{N}$ -labelled protein sample we obtained virtually complete assignment of the  $^1\text{HN}$ ,  $^1\text{Ha}$ ,  $^{13}\text{C}$ ,  $^{13}\text{Ca}$ ,  $^{13}\text{Cb}$  and  $^{15}\text{N}$  resonances in DFPase. In addition to standard [ $^{15}\text{N}$ ,  $^1\text{H}$ ]-TROSY type triple-resonance experiments,  $^1\text{Ha}$ -based triple-resonance pulse sequences, such as HCACO, HCACB, (HCA)CO(CA)NH and H(CA)NH were employed, taking advantage of  $^1\text{Ha}/^{13}\text{Ca}$  multiple-quantum line-narrowing to improve  $^{13}\text{Ca}$  relaxation properties. The efficiency of all experiments performed is amino-acid type specific due to variations in the Ca deuteration level. In this respect HN- and Ha-directed experiments were found to complement each other.

## Quantification Of $^1\text{H}$ NMR Blood Serum Lipoprotein Spectra In Stroke And In Alzheimer's Disease. A Preliminary Comparative Study

*Vincenzo Lombardi<sup>1</sup>, Tibor Lipta<sup>2</sup>, Rainer W. Wechselberger<sup>3</sup>, Nico van Nuland<sup>3</sup>, Emerich Majer<sup>4</sup>, Jaroslava Budinska<sup>5</sup>, and Antonio Troncone<sup>1</sup>.*

<sup>1</sup>Institute of Pathological Anatomy, University of Bari, Italy

<sup>2</sup>Faculty of Chemical Technology, Slovak Technical University of Bratislava, Slovakia.

<sup>3</sup>Department of NMR spectroscopy, University of Utrecht, Netherlands.

<sup>4</sup>Department of Pathology, Institute of Psychiatry, Prague, Czech Republic.

<sup>5</sup>Department of Neurology, Litomerice Medical Center, Czech Republic.

The etiopathology of Alzheimer's disease (AD) is still unknown after innumerable studies and publications.

However, beyond the genetic factors, which are not considered causative, there is evidence, more and more, that cerebrovascular atherosclerosis with lipoproteins alterations is one of risk factors in stroke and AD. This preliminary comparative study is the first attempt reported in the literature to quantify the  $^1\text{H}$  NMR spectra of lipoprotein fractions of blood serum of stroke and AD. Based on the previous Proton Nuclear Magnetic Resonance Spectroscopy ( $^1\text{HNMRS}$ ) analysis of blood plasma lipoprotein in coronary heart occlusion, we have carried out the COMPARATIVE STUDY of the blood serum lipoprotein fractions VLDL, LDL and HDL of patients with vascular-atherosclerosis-stroke of various degree and patients with Alzheimer's disease (AD) compared to normal healthy subjects. We applied the line shape fitting analysis with mathematical separation of the overlapping resonances from the VLDL, LDL and HDL. HDL was decreased in stroke and more dramatically decreased in AD. LDL was increased in stroke and in AD while VLDL was increased in stroke and poorly detected in AD. Higher content of macromolecules and of some amino acids were found in the aliphatic region only in the blood serum of AD. Although this is only a limited preliminary investigation, it might suggest that the AD & stroke have some etiopathological factors of arteriosclerosis in common and further studies are worthwhile for differential analysis of lipoproteins in both diseases. This investigation confirms the potential role of  $^1\text{HNMRS}$  quantification analysis of lipoproteins with more rapidity and accuracy than the routine lipid testing.

## Expression and characterisation of the natively unfolded membrane translocation domain of colicinE9

*Kaeko Tozawa, Colin J. Macdonald, Emily S. Collins, Richard James, Christopher Penfold, Geoffrey R. Moore*

ColicinE9 is a member of a family of antibacterial proteins produced by *E. coli* that kills target cells by degrading their DNA in the cytoplasm. The protein must be translocated across the outer and inner membranes to express its toxicity. It consists of three domains; translocation (T), receptor-binding (R) and DNase domains. We showed that only the first 83 residues of the T-domain in the intact colicinE9 gave signals in 15N-HSQC spectra, indicating that the N-terminal region of the T-domain is flexible and disordered. We also showed that the disordered region contained the binding epitope for TolB, a periplasmic protein in the target cell that helps in translocation, and that parts of the TolB bound T-domain remained disordered. In order to complete the signal assignment and to characterise fully features of the TolB binding epitope, the N-terminal 61 amino acid residues of the T-domain (T61) were expressed in *E. coli* as a 25kDa fusion protein with E9DNase.

The HSQC spectrum shows relatively sharp signals of residues 5-61 from the T-domain and the 8-residue linker region and broader signals from the E9DNase domain. To date 48 of 69 NH signals of the T61 and linker regions have been assigned and 15N T1, T2 and 1H-15N NOE measurements made. T1 values were similar throughout, while the N-terminus has a longer T2 and the TolB box and its C-terminal region had shorter T2 values. Hence the T1/T2 ratio of the residues 39-47 is larger, indicating the mobility of this region is limited. Consistent with this was the concurrent observation of smaller 1H-15N NOE's. These results suggest that the TolB box and its C-terminal region are slightly more ordered in this generally disordered region. The unique feature of this region may be involved in the translocation mechanism of molecules across the membrane.

Alanine mutants of the TolB box residues Asp-35 and Trp-39, essential for activity were prepared to determine the effects of these important residues on the ordering within its TolB box. Characterisation of the mutants will be presented.

## An NMR study of blue shifted intermediates of the photoactive yellow protein

*D.R.A. Marks, N.M.Derix, M.A. van der Horst, N.A.J. van Nuland, R. Boelens, K.J. Hellingwerf, R. Kaptein*

The photoactive yellow protein (wt-PYP) is a small 14kD water soluble protein which undergoes a photocycle at a time scale of ~500ms. It was previously shown from NMR data that the protein structure is altered during the photocycle, as many cross-peaks vanish in the blue shifted intermediate (pB) due to broadening. In particular the N-terminal part of the wt-PYP seems to become detached from the protein mass.

We investigated a derivative of wt-PYP (*f'*25-PYP) of which 25 residues from the N-terminal were removed. *f'*25-PYP undergoes a similar photocycle, though the photocycle recovery time is in the order of 10 minutes. The long lifetime makes *f'*25-PYP suitable for determination of the structure of the pB state. For example, it is possible to assign most crosspeaks in the pB state of this protein. It was also observed that the temperature stability of *f'*25-PYP has suffered as result of the removal of the N-terminal. It is notable that the pattern of the temperature induced instability in *f'*25-PYP ground state (pG) corresponds well with the broadening observed in the pB state of the wt-PYP.

## Are Efficient Contrast Agents Ready for Use at Very High Field Imaging ?

*Robert N. Muller*

NMR Laboratory, Department of Organic Chemistry, University of Mons- Hainaut, B-7000 Mons, Belgium

In the future, many aspects of the biomedical MR research will be carried out at high and very high magnetic fields (i.e.  $B_0 > 4T$ ), a range in which most of today's paramagnetic contrast agents exhibit poor relaxivities.

New approaches are requested which exploit theories and parameters overlooked so far, like the beneficial influence of long water exchange time of dysprosium chelates.

In this new context also, the transverse relaxivity has to be considered rather than the longitudinal one, and consequently, negative contrast agents could become the standards. Among those, the superparamagnetic particles seem to be very promising particularly in the domain of cellular and molecular imaging.

## The extracellular domains of the signaltransducer gp130

*Michael Pachta-Nick, Rainer Wechselberger, Nico van Nuland, Joachim Grötzinger*

Glycoprotein 130 (gp130) is a type I transmembrane protein and serves as the common signal-transducing receptor subunit of the interleukin-6-type cytokines. Whereas the membrane-distal half of the gp130 extracellular part confers ligand binding the structural and functional features of its membrane-proximal half are poorly understood. On the basis of predictions of tertiary structure, the membrane-proximal half consists of three fibronectine-type-III-like domains D4, D5 and D6. However, to gain certainty and to understand the relation between structure and function it is necessary to solve its structure, for instance by NMR spectroscopy.

We expressed the recombinant single domains D4, D5 and D6 and two constructs consisting of the coupled domains D5 and D6, D3 and D4, respectively. While the three single domains turned out to be relatively unstable particularly regarding temperature and concentration, the two double domains are easy to handle. After purification and concentration of the double domain D56 the triple resonance NMR spectra were recorded and used for the sequential assignment of this 25 kDa protein.

## The Solution Structure of the Imaging Agent <sup>111</sup>In-Bleomycin Complex Studied by NMR and Molecular Modelling

*Athanasios Papakyriakou, Nikos Katsaros*

The bleomycins (BLMs) are a multitudinous group of glycopeptide derived natural products isolated from *Streptomyces verticillus* and are clinically used in the treatment of several neoplastic diseases. In the presence of the cofactors Fe(II) and O<sub>2</sub> this drug has the ability to mediate DNA single and double strand scissions, with the latter thought to be the principal locus of their cytotoxicity. A variety of metal ions have been used as radiolabeling imaging agents in combination with BLM, such as Co-57, Ga-67, Tc-99m and In-111. Most of them have failed either because of lack in vivo stability or tumor affinity. However, In-111 has shown to form a stable complex with BLM at low pH which did not demonstrate any affinity for transferrin and exhibited very high sensitivity and specificity in head and neck cancer patients.

By means of NMR studies we have found that In(III)BLM complex formed at low pH is also stable under physiological conditions. Employing 2D NMR experiments we are in progress of the structural characterization of the complex formed, in combination with molecular dynamics calculation carried out with the Amber force field. Sequence specific interaction with DNA will be carried out with synthetic oligonucleotides that will reveal the mode of binding to the main target of these drugs.

## Paramagnetic Constraints In Structure-Determination Programs

*Ivano Bertini, Claudio Luchinat, Giacomo Parigi*

In proteins containing paramagnetic metal ions a new class of constraints for solution structure determination can be obtained: the paramagnetism-based constraints. Paramagnetism-based constraints are the contact shifts, the pseudocontact shifts (PCS), the hyperfine shifts as sum of the two, the relaxation enhancements, and the cross-correlation between Curie spin relaxation and dipole-dipole nuclear relaxation. Residual dipolar coupling (RDC) can also arise from the presence of a paramagnetic ion. All such constraints have been incorporated in the program PARAMAGNETIC DYANA over the years.

Paramagnetism-based constraints are much quicker to be obtained than the classical NOE constraints, especially for large size proteins. In fact, NOEs become more and more difficult to be determined with the protein size. Therefore, the development of new methods, independent of the measurement of NOE, or at least of the measurement of a large number of them, is of great importance in order to increase the speed in solving protein structures and to obtain structures of large proteins.

## <sup>1</sup>H NMRD measurements

Ivano Bertini<sup>a</sup>, Marco Fraga<sup>a</sup>, Claudio Luchinat<sup>a</sup>, Kirill Nerinovski<sup>a</sup>, Giacomo Parigi<sup>a</sup>

<sup>a</sup>Magnetic Resonance Center, University of Florence, Via L. Sacconi, 6, 50019 Sesto Fiorentino, ITALY

Nuclear Magnetic Relaxation Dispersion (NMRD) is a well established technique to obtain information on molecular dynamics in biological systems, through the correlation times of different kind of motions, and also to refine the structural data, as relaxation depends on the presence and the distance of protons coordinated to the metal center, which is often the active site of proteins. In last few years the growing interest in application of this technique to the investigation of the proteins in solid and semisolid states through the direct observation of the NMR signals of protein protons puts forward the new demands to the experimental machines with increased sensitivity and ability to measure signals with very fast relaxativity. A set of experiments on different samples, from very low to very high relaxation rates, have been performed, in order to test the linearity of the rate with paramagnetic ion concentration, to check the agreement between Stelar and Koenig-Brown relaxometers, to monitor the reliability of the measurements in the wide available magnetic range, and to test its sensitivity. All these tests allowed us to optimize the data acquisition protocols, and thus the relaxation measurements on the following systems.

<sup>1</sup>H NMRD measurement were performed on the complex Gd-DOPTA, a possible contrast agent for MRI. The design of this contrast agent was based on the mechanism of inner sphere relaxation coupled with a Ca<sup>2+</sup>-dependent conformational switch. In short, the accessibility of water molecules to the bound Gd<sup>3+</sup> ions and hence the relaxivity of DOPTA-Gd are controlled by Ca<sup>2+</sup> concentration. Relaxometric measurements confirm this behavior and provide an indication that second sphere water-molecules are probably responsible for paramagnetic relaxation enhancement in the absence of Ca<sup>2+</sup>. After Ca<sup>2+</sup> is bound to DOPTA-Gd, the molecule undergoes a substantial conformational change that opens up the hydrophilic face of tetraazacyclododecane macrocycle. This change dramatically increases the accessibility of chelated Gd<sup>3+</sup> ion to bulk solvent.

The relaxometric properties of biotinylated paramagnetic liposomes with different lipophilic complexes have been investigated by <sup>1</sup>H NMRD. The proton relaxivity was found to have a peak at the proton Larmor frequencies generally used in MRI, and to be largely affected by the residence lifetime of the water molecule in the coordination site of the metal chelate. The measurements also indicate that a local motion in the nanosecond time scale, i.e. much faster than the rotational time of the whole liposome, is effective. Conjugation of liposomes of this type with antibodies directed towards receptors over-expressed in tumor cells is being tested as a possible strategy for early detection of cancer by MRI.

Protein hydration studies are another field of application of <sup>1</sup>H NMRD. Oxidized rubredoxin showed an increased water <sup>1</sup>H relaxation profile with respect to the diamagnetic gallium derivative or reduced species. Analysis of the data shows evidence of exchangeable proton(s) around 4.0-4.5 Å from the metal ion. The correlation time for the proton-electrons interaction is  $7 \times 10^{-11}$  s and is attributed to the effective electron relaxation time. Analogous relaxation measurements were performed on the C6S rubredoxin variant, whose iron(III) center has been previously shown to be coordinated to three cysteine residues and a hydroxide ion above pH 6. <sup>1</sup>H NMRD profiles indicate increased hydration with respect to the wild type. This may account for the difference in reduction potential of the C6S variant with respect to the other CtoS mutants, as increased solvent accessibility is expected to favor the more highly charged reduced state  $[\text{Fe}^{\text{II}}\text{S}_3\text{O}]^{2-}$ .

## Conformational analysis of a chemosensory protein from *Scistocerca gregaria*

D. Picone, S. Tomaselli, O. Crescenzi, T. Tancredi, R. W. Wechselberger and, R. Boelens

Chemosensory proteins (CSPs) are a class of small soluble proteins present at high concentration in the chemosensory organs of different insect species, that are supposed to be involved in carrying the chemical messages from the environment to the chemosensory receptors. However, a structural basis for the mechanism of delivery is still lacking. In order to provide a detailed conformational characterisation of a member of this class of proteins, we cloned a specific isoform (CSP-sg4) from *S. gregaria* and expressed it in *E. coli* (1). The recombinant protein was found to be identical to the native one with respect to pairing of the disulphide bridges, aggregation state and secondary structure elements. CD spectra of both native and recombinant protein are essentially identical, and show features typical of a predominantly helical fold, with a characteristic double minimum at 208 and 220 nm, which displays a remarkable stability with respect to variations in temperature and pH (2). A preliminary NMR study confirms the presence of a folded structure, with amide protons ranging from 9.5 to 6.8 ppm, and some side-chain signals resonating at large negative deltas (up to -1.35 ppm). The high helical content inferred from CD is confirmed by the pattern of NOEs, such as the large number of strong HN-HN contacts. So far we have achieved the assignment of 90% of the backbone <sup>1</sup>H and <sup>15</sup>N resonances. A full structural characterization of this protein using 3D NMR data is currently in progress at the European LSF for Biomolecular NMR in Utrecht.

### References

1. Angeli S et al. (1999) Eur. J. Biochem. 262, 745-754.
2. Picone, D. et al (2001) Eur. J. Biochem. 268,4794-4801.

## A Simple Protocol To Study Blue Copper Proteins By NMR

Ioannis Gelis‡, Nikolaos Katsaros‡, Claudio Luchinat§, Mario Piccioli^\*, Luisa Poggi^

‡ NCSR Demokritos, Institute of Physical Chemistry, 15310 Agia Paraskevi Attikis, Greece.

§ Magnetic Resonance Center and Department of Agricultural Biotechnology, University of Florence, Italy.

^Magnetic Resonance Center and Department of Chemistry, University of Florence, Italy

An NMR approach based on classical two and three dimensional experiments for sequential assignment leaves unobserved in the case of oxidized plastocyanin from *Synechocystis* sp. PCC6803 14 residues out of 98 amino acids. A protocol that simply makes use of tailored versions of 2D HSQC and 3D CBCA(CO)NH and CBCANH leads to the identification of 9 of the above 14 residues. At variance with previous approaches, the proposed protocol does not involve the use of unconventional experiments designed specifically for paramagnetic systems, and does not exploit the occurrence of a corresponding diamagnetic species in chemical exchange with the blue copper form. This protocol is expected to extend the popularity of NMR in the structural studies of copper (II) proteins, because it allows researchers to increase the amount of information available via NMR on the neighborhood of a paramagnetic center without requiring a specific expertise in the field. The resulting 3D spectra are standard spectra that can be handled by any standard software for protein NMR data analysis.

## Semi-automatic stereospecific resonance and NOESY assignment of proteins based on the tertiary structure - the program nmr2st

<sup>1</sup>Primož Pristovšek, <sup>2</sup>Lorella Franzoni and <sup>3</sup>Heinz Rüterjans

<sup>1</sup>National Institute of Chemistry, Hajdrihova 19, SI-1000 Ljubljana, Slovenia;

<sup>2</sup>Department of Experimental Medicine - Section of Chemistry and Structural Biochemistry, University of Parma, 43100 Parma, Italy;

<sup>3</sup>Institute of Biophysical Chemistry, G.W. Goethe University of Frankfurt, 60439 Frankfurt, Germany.

The present trend of structural genomics and protein folding, as well as many studies by NMR (e.g., SAR) have placed high demands aiming at fast results. Many efforts have been made to automate several steps of NMR data analysis, e.g. resonance assignments, NOE assignments and structure determination. Most of the developed softwares are reviewed in ref. 1, followed by others that were more recently described (2-4).

In the course of work in our labs the need has arisen for machine assistance in sequence-specific and NOESY cross-peak assignment that would maintain full human expert control over all data at all times and would use computer speed and precision only in well-defined stages of the process providing output for the next stage. In this way manual correction and addition or deletion of data, that is often erroneously handled by fully automatized procedures, is possible at any point providing a more reliable and accurate final result. For this purpose we have developed the program package st2nmr (from structure to NMR) for semi-automatic sequence-specific assignment (5).

In the present work we present the nmr2st (from NMR to structure) program for semi-automatic NOESY assignment. It contains a set of tools for NMR structure refinement that prepares NOE distance restraint lists for structure calculation programs providing hyper-linked displays of possible assignments for each peak, taking advantage of a 3D model if present. Additionally, structure ensembles created by structure calculation programs can be analysed with nmr2st providing suggestions for changes in the restraint list. The preliminary version of the program has been successfully used in our labs (6-8). We are currently developing a module that provides stereospecific assignments of prochiral groups using the NOESY cross-peaks based on the tertiary structure of the protein before the final structure calculation is started. It was established rather early that stereospecific assignments are essential for obtaining high-quality NMR structures with low r.m.s.d. values of the ensembles (9). An error in stereospecific assignment, however, may lead to inaccurate positions of the side-chains in the final structure; strict protocols for accepting a stereospecific assignment are therefore essential.

### References

- (1) H.N. Moseley and G.T. Montelione (1999) *Curr. Opin. Struct. Biol.*, 9, 635-642
- (2) M. Assfalg, I. Bertini, P. Turano, M. Bruschi, M.C. Durand, M.T. Giudici-Ortoniconi and A. Dolla (2002) *J. Biomol. NMR*, 22, 107-122
- (3) N. Oezguen, L. Adamian, Y. Xu, K. Rajarathnam and W. Braun (2002) *J. Biomol. NMR*, 22, 249-263
- (4) T. Herrmann, P. Güntert and K. Wüthrich (2002) *J. Mol. Biol.*, 319, 209-227
- (5) P. Pristovšek, H. Rüterjans and R. Jerala (2002) *J. Comput. Chem.*, 23, 335-340
- (6) P. Pristovšek, C. Lücke, B. Reincke, B. Ludwig and H. Rüterjans (2000) *Eur. J. Biochem.*, 267, 4205-4212
- (7) B. Reincke, C. Pérez, P. Pristovšek, C. Lücke, C. Ludwig, F. Löhr, V. Rogov, B. Ludwig and H. Rüterjans (2001) *Biochemistry*, 40, 12312-12320
- (8) L. Franzoni, C. Lücke, C. Pérez, D. Cavazzini, M. Rademacher, C. Ludwig, A. Spisni, G. L. Rossi and H. Rüterjans (2002) *J. Biol. Chem.*, 277, 21983-21997
- (9) P. Güntert, W. Braun, M. Billeter and K. Wüthrich (1989) *J. Am. Chem. Soc.*, 111, 3997-4004

**Acknowledgements:** The European Large Scale Facility for Biomolecular NMR at the University of Frankfurt (Germany) is gratefully acknowledged for the use of its equipment.

## Development of a quadruple hyphenated HPLC-DAD-radical scavenging detection-NMR system for the rapid identification of antioxidants in complex plant extracts

*A. Pukalskas, T. A. van Beek, P. de Waard, P. R. Venskutonis*

There is a considerable interest in recent years in finding new natural antioxidants for possible use in foods and other applications. Rosemary and sage extracts are used as such. Mostly complex crude plant extracts are screened for antioxidant activity. However, such screening tests do not yield information about the activity of individual compounds. Recently an HPLC on-line radical scavenging methods providing an indication about the activity of separate peaks were developed. Thus, it is no longer necessary to isolate and purify each compound. One can "zoom" in on the active peaks. The principle of such methods is based on the post-column addition of a relatively stable radical (DPPH or ABTS), which is reduced when phenols elute. All known powerful natural antioxidants are also radical scavengers. Still when active compounds have been found, they need to be identified. Then time-consuming and difficult separations are necessary which diminishes some of benefits of on-line screening. Also some antioxidants decompose easily which greatly complicates their purification. By combining LC-NMR with on-line antioxidant screening we tried to both determine the activity and elucidate the structure of active compounds without any laborious purification steps or risk of decomposition.

The set up of an on-line DPPH method before linking it to NMR was modified as follows: the flow from the HPLC column was split into two parts, one, at a rate of 0.2 ml/min was passed to DPPH reaction coil. A 4.4 m length 0.1 mm i.d. peek tubing was used as reaction coil. DPPH solution (10<sup>-4</sup> M) was added to the reaction coil by syringe pump at a flow rate 0.5 ml/min. Decrease of the absorbance of DPPH solution was monitored by visible light detector at 517 nm.

The other part of the flow was passed to solid phase extraction equipment "Prospect 2" at a rate of 0.6 ml/min. Ultra pure water was added into an HPLC solvent stream at a flow rate 0.4 ml/min straight after the splitter. This mixture was then passing DAD and "Prospect 2".

The method was tested using commercial rosemary extract "RBT 257". All major peaks appearing in the HPLC chromatogram were trapped on a special cartridges.

After the separation being completed the cartridges with trapped compounds were dried in a nitrogen stream. By comparing DPPH scavenging and DAD chromatogram profiles the activities of separate peaks were determined and the compounds, having DPPH radical scavenging activity were eluted from the cartridges with deuterated methanol and delivered to the LC-NMR 250 ml measuring cell. <sup>1</sup>H NMR spectra were recorded on a Bruker 400 DPX instrument. For the major compounds 2D COSY and TOCSY spectra were recorded, and for the compound, present at the highest concentration it was possible to record an HMBC spectrum.

The major compounds in the investigated rosemary extract were identified as carnosol and carnosic acid, by comparing their <sup>1</sup>H NMR spectral assignments with those found in literature. Although other compounds have not been yet identified, their spectral data provide an important information about their structures. This information in combination with MS data, which was recorded from the solutions collected after NMR measurements, is sufficient to identify at least some of them. The conclusion is that the combination of selected in this study methods or variations thereof can be used in high-throughput screening of crude plant extracts.

## Structural and folding studies on calycons: beta-lactoglobulins and chicken liver basic fatty acid binding protein

*Laura Ragona, Francesca Vasile, Raffaella Ugolini, Lucia Zetta, Hugo Monaco and Henriette Molinari*

The lipocalins, the fatty acid binding proteins (FABP) and the avidins are three families of hydrophobic ligand binding proteins which together form the calycin superfamily. Lipocalins and FABPs share a related beta-barrel structure. Lipocalins are mostly extracellular proteins displaying a wide variety of biological functions, while FABPs are predominantly intracellular proteins involved in the lipid metabolism. Beyond some functional similarities (hydrophobic ligand binding) these families are characterised by a similar folding pattern (an anti-parallel beta barrel dominated by a largely +1 topology), within which large parts of their structures can be structurally equivalenced, although the families share no global sequence similarity.

We have investigated and are investigating the structural, folding and binding properties of beta-lactoglobulins from different species, which are important representatives of the lipocalin family. Recently we have undertaken the structural characterisation of Chicken Liver Basic FABP, belonging to the basic type FABPs.

A comparative analysis of the structural, folding and interaction properties of these proteins is currently in progress in our laboratory and will be presented here.

## The effects of domain dissection on the folding and stability of the 43kDa protein, PGK

*Michelle A. C. Reed, Andrea M. Hounslow, Anthony R. Clarke, C. Jeremy Craven and Jonathan P. Waltho*

The characterisation of early folding intermediates is key to understanding the protein folding process. Previous studies of the N-domain of phosphoglycerate kinase from *Bacillus stearothermophilus* combined equilibrium amide exchange data with a kinetic model derived from stopped flow kinetics. Together these implied the rapid formation of an intermediate with extensive native-like hydrogen bonding. However, there was an absence of protection in the region proximal to the C-domain in the intact protein.

A question arises: Is this absence of protection due to local unfolding events caused by the absence of the C-domain, or does it reflect the local, rather than global, nature of the N-domain kinetic intermediate? We have addressed this issue using stopped flow kinetics and amide exchange data after obtaining the prerequisite backbone assignment of the intact 43 kDa PGK molecule using perdeuteration and a TROSY-based suite of experiments.

## Three State Model for Watson-Crick Base Pairing in DNA and Experimental Dissection of Free Enthalpies of Stacking and Hydrogen Bonding

*Harald Schwalbe, Christian Richter, Christian von der Heyden, Christian Griesinger*

A second topology of Watson-Crick base pairs in standard B-form DNA has been determined from analysis of the field dependence of  $^1\text{H}$  line width of imino hydrogen atoms by NMR spectroscopy. The second topology is distinct from the usual hydrogen bonded form but also distinct from the topology in which imino and amino hydrogen atoms exchange with water. Quantum chemical calculation and molecular dynamics simulations show that the hydrogen bonds are dislocated by less than 5pm. Such small dislocation will preserve the stacking interaction between neighboring nucleobases. Populations of the base pair open form and the new intermediate form have been determined to be  $10^{-5}$  and  $10^{-2}$ , respectively. These populations form a basis to dissect the contribution of stacking and hydrogen bonding and their variation along the oligonucleotide in standard B-form DNA to the stability of Watson-Crick base pairs on the assumption that stacking interactions are preserved in the intermediate conformation.

## Effect of cations and ash on solid state NMR spectra.

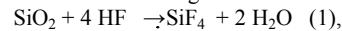
*Barbara Scaglia<sup>1</sup>, Fabrizio Adani<sup>1</sup>, Fulvia Tambone<sup>1</sup>, Adrie de Jager<sup>2</sup>, Adrie Veeken<sup>3</sup>.*

<sup>1</sup>DiProVe, Fac. di Agraria, Università degli Studi di Milano, Via Celoria 2, 20133 Milano Italy.

<sup>2</sup>Lab. of Biophysics, Wageningen University, Dreijenlaan, 36703 HA, Wageningen The Netherlands.

<sup>3</sup>Dep. of Environmental Technology Wageningen University, P.O. Box 8129, 6700 EV Wageningen, The Netherlands.

In principle, solid state N.m.r. spectroscopy offers attractive perspectives for investigating the chemical structure of soil organic matter without the chemical manipulation of the sample. However, this technique is limited by two factors, i.e. that the concentration of organic matter in soil is very low (ca. 3 % w/w), whereas the concentration of ferric cation is relatively high (3-4 %), and this yield poor quality badly resolved spectra. It is well known that ferric cation and most other cations are water soluble as chlorides, and thus treating of soil samples with aqueous HCl only should allow obtaining cation free soil matter in H<sup>+</sup> form (product 1). It is also known that concentrated HF dissolves silicon oxide according to reaction 1



and thus treating of cation free soil samples with HF should allow to make soluble the whole inorganic matter and to separate it from the acid insoluble organic matter.

In order to set up an analytical procedure to improve N.m.r. resolution five different samples, amended with compost, slurry and manure, were taken from different locations in North Italy. The objective of this work is to record and interpret the solid state N.m.r. spectra of untreated soil (thesis A), treated soil with HCl (thesis B) and treated with HCl + HF (thesis C) according to previous work and to assess the effects of acid treatment on spectral quality and/or significance, and hopefully on the nature of the starting soil organic matter. During the treatments with HCl (thesis B) the concentration of cations Al, Mg, Ca, Na, K and Fe were monitored in the acidic solution by AAS. On the other hand during the treatment with HCl+HF ashes concentration was monitored. During all treatment complete mass balance for total solids, volatile solids and organic carbon were made both from a relative that absolute point of view. Qualitative and semiquantitative data were obtained.

Comparing the spectra of thesis A, B e C for each soil sample we can see that treatment with HF improved the quality of the spectra. Also the treatment with HCl improved the quality of spectra but less. This was due, probably to the less carbon content and suggested that N.m.r. spectra quality, depended both by C content that paramagnetic cation contents. Nevertheless, mass balance suggested that treatment with HCl+HF determined carbon losses that should be taken into account when N.m.r. spectra are used to describe the composition of organic matter in bulk soils.

Literature suggested in the past the use of HF to improve the quality of C-NMR spectra, but, did not reported any data about C losses from an absolute point of view. Therefore this lack of information did not help researcher to well investigate about organic carbon in bulk soils, giving erroneous interpretation.

Next step of the research will be the improvement of HCl treated spectra, by N.m.r. parameters (acquisition time, pulse sequence etc.) in order to obtain satisfy spectra and conserving soil C.

## Cerebral Perfusion Imaging by Pulsed Arterial Spin Labeling

*Janneke Schepers and Klaas Nicolay*

Magnetic Resonance Imaging (MRI) allows for the measurement of cerebral blood flow (CBF) by exogenous and endogenous contrast-enhanced methods. Exogenous contrast-enhanced perfusion MRI requires the injection of a paramagnetic contrast agent, usually a gadolinium chelate. Endogenous contrast perfusion MRI relies on the magnetic labeling of arterial water with respect to tissue water. For endogenous contrast-enhanced perfusion MRI, two methods have been developed: continuous arterial spin labeling (CASL) and pulsed arterial spin labeling (PASL), which differ in the way the arterial water is labeled. We have implemented the flow-sensitive alternating inversion recovery (FAIR) technique for CBF measurements in healthy and ischemic rat brain. The aims of our work were threefold: i) to identify hemodynamic and experimental parameters that affect quantification of CBF by FAIR imaging; ii) to adapt the FAIR technique, such that CBF quantification can be improved; and iii) to compare FAIR perfusion imaging to contrast-enhanced perfusion MRI in different experimental models of cerebral ischemia in rat brain. This presentation will give an overview of our results.

## Structure Refinement of a DNA Hairpin Using Very Small Residual Dipolar Couplings

Petr Padrta, Lukas Zidek, Richard Stefl, and Vladimir Sklenar

Number of one-bond  $^1\text{H}$ - $^{13}\text{C}$  and  $^1\text{H}$ - $^{15}\text{N}$  spin pairs in adenine, guanine, thymine, uracil, and cytosine bases, which supply sufficiently large residual dipolar couplings, is limited to just a few. In addition to one-bond RDCs also two-bond interactions may provide important source of restraints for structure refinement in nucleic acids. In purine and pyrimidine bases, a number of two-bond and one-bond homo and heteronuclear distances has a well-defined length and can be successfully used during the structure calculations. As will be shown, a suite of spin-state-selective excitation (S3E) NMR experiments can be successfully employed for the measurements of small residual dipolar one-bond ( $^{13}\text{C}$ - $^{13}\text{C}$ ,  $^{13}\text{C}$ - $^{15}\text{N}$ ) and two-bond ( $^1\text{H}$ - $^{13}\text{C}$ ,  $^1\text{H}$ - $^{15}\text{N}$ ) coupling constants. Scalar and residual dipolar couplings were measured in the  $^{13}\text{C}$ ,  $^{15}\text{N}$ -labeled DNA hairpin d(GCGAAGC) with very high precision and accuracy. Both "classical" NMR restraints and a set of residual dipolar couplings were used in the structure refinement of this DNA hairpin.

## Scorpion toxin TsTX-IV: solution structure, pH dependence of molecular flexibility and docking on the $\text{K}^+$ channel

<sup>1</sup>L. Franzoni, <sup>2</sup>P. Pristovšek, <sup>3</sup>S. Oyama Jr., <sup>3</sup>T.A. Pertinhez, <sup>4</sup>C. Lücke, <sup>5</sup>E. Schininà, <sup>6</sup>E.C. Arantes, <sup>4</sup>H. Rüterjans and <sup>1,3</sup>A. Spisni

<sup>1</sup>Dept. of Experimental Medicine - Sect. of Chemistry and Structural Biochemistry, University of Parma, Italy; <sup>2</sup>National Institute of Chemistry, Ljubljana, Slovenia; <sup>3</sup>BioNMR Lab, CeBiME-LNLS, Campinas, Brazil; <sup>4</sup>Inst. of Biophysical Chemistry, J.W. Goethe University of Frankfurt, Germany; <sup>5</sup>Dept. of Biochemical Sciences, University of Roma, Italy; <sup>6</sup>Dept. of Physics and Chemistry, USP-RP, Ribeirão Preto, Brazil

Scorpions represent a considerable public health problem in many countries and their venoms and respective toxins have been widely investigated as suitable tools for pharmacological and electrophysiological studies, mainly those concerned with their effect on ion channels. In Brazil, many cases of accidents involving scorpion envenomation are caused by *Tityus serrulatus*. The fractionation of its venom gives more than a dozen of bioactive polypeptides, named tityus toxins (TsTX). Among them, TsTX-IV represents a novel eight-cysteine neurotoxin characterized by the ability to inhibit the high conductance  $\text{Ca}^{2+}$ -activated  $\text{K}^+$  channels (1).

Using mass spectrometry, besides determining the disulfide bridge pairings, we found that, differently from what previously reported (1), the toxin sequence coincides with the one of butantoxin (2).

The solution structure of TsTX-IV consists of a small triple-stranded antiparallel  $\beta$ -sheet anchored to a short  $\alpha$ -helix by two disulfide bridges, resulting in a  $\beta\alpha\beta\beta$  motif. Although the  $\alpha\beta$  scaffold is conserved among other known short-chain scorpion toxins, some structural differences can be identified. The NMR data collected at different pH values suggested an increase in molecular flexibility by increasing the pH from 4.5 to 6.0. This observation has been confirmed by molecular dynamics calculations.

Selected structures of the toxin from the MD trajectories obtained at the two pHs were docked on a model of the Shaker B  $\text{K}^+$  channel constructed by homology modeling on the basis of the crystal structure of KcsA (3). Both the localization of key residues responsible for the binding and the role that pH may play in modulating the toxin-channel complex formation will be discussed.

### References

- (1) Novello, J.C., Arantes, E.C., Varanda, W.A., Oliveira, B., Giglio, J.R., Marangoni, S. (1999) *Toxicon* **37**, 651-660
- (2) Holaday, S.K., Martin, B.M., Fletcher Jr., P.L., Krishna, N.R. (2000) *Arch. Biochem. Biophys.* **379**, 18-27
- (3) Doyle, D.A., Morais Cabral, J., Pfuetzner, R.A., Kuo, A., Gulbis, J.M., Cohen, S.L., Chait, B.T., MacKinnon, R. (1998) *Science* **280**, 69-77

### Acknowledgements

Partly supported by MIUR, CNR (Italy) and FAPESP (Brazil). The European Large Scale Facility for Biomolecular NMR at the University of Frankfurt (Germany) and the Center for Structural and Molecular Biology of the National Lab. of Synchrotron Light (CeBiME-LNLS) at Campinas (Brazil) are acknowledged for the use of their equipment.



**NMR and Molecular Dynamic Studies of Agonist and Antagonist Peptides of the Guinea Pig Myelin Basic Protein Epitope 74-85 in Solution: Comparison with a Homology Model Reconstruction of the Integral Protein and Implication for Structure-Function Relationship.**

*Andreas G. Tzakos, Patrick Fuchs, Anastasios Troganis, Theodore Tselios, Nico A.J. van Nuland, Spyros Deraos, John Matsoukas, Ioannis P. Gerotheranassis and Alexandre M.J.J. Bonvin*

Experimental allergic encephalomyelitis (EAE, the animal model of Multiple Sclerosis) is induced in susceptible animals by immunodominant determinants of myelin basic protein (MBP), such as the guinea pig epitope MBP74-85. In order to characterize the molecular features of antigenic sites we report detailed  $^1\text{H}$  and  $^{13}\text{C}$  NMR chemical shift assignments, 2D  $^1\text{H}$ - $^1\text{H}$  NOESY experiments, conformational properties and molecular dynamic analysis (MD) of two potent linear dodecapeptide analogues of the guinea pig MBP74-85. The two analogues Gln74-Lys75-Ser76-Gln77-Arg78-Ser79-Gln80-Asp81-Glu82-Asn83-Pro84-Val85 (MBP74-85) and Gln74-Lys75-Ser76-Gln77-Arg78-Ser79-Gln80-Ala81-Glu82-Asn83-Pro84-Val85 (Ala81MBP74-85), which induce and inhibit respectively Experimental Autoimmune Encephalomyelitis, differ only in the aminoacid residue at position 81 (Asp or Ala), however, they result in relatively different side-chain and backbone folded conformations. Restricted Molecular dynamics based on NOE constrains indicate the close proximity of Arg78 / Asp81 side chain in DMSO and Lys72 / Asp81 in aqueous solution for the agonist MBP74-85. Both interactions are absent in the case of the antagonist Ala81 MBP74-85, which may account for the triggering of the disease. The structure of the integral guinea pig MBP based on homology modeling is also reported in an attempt to localize certain post-translational modifications relevant to multiple sclerosis, such as the reduction in cationicity of MBP, especially due to conversion of positively charged arginine residues to uncharged citrulline.

**NMR Studies Of The Reaction Products Obtained By Reducing Chromate With A Bovine Liver Extract**

*Elena Gaggelli, Nicola D'Amelio, Nicola Gaggelli, Francesca Mancini, Elena Molteni, Daniela Valensin, Gianni Valensin*

NMR data are presented which, together with other spectroscopic data, shed light on species occurring in solution when sodium chromate is reacted with a bovine liver extract. In spite of well-established data reported in the literature, evidence is provided of the occurrence of a complicated mixture of Cr(V) complexes. The analysis of paramagnetic shifts, of their temperature dependence and of TOCSY and ROESY data allows to identify some moieties bound to the chromic ion. Evidence is thus provided of two diverse His residues and two asp and glu moieties which are coordinated to Cr(V).

## Measuring Flow And Vessel Wall Permeability In Plants Using MRI

C.W. Windt, F.J. Vergeldt, P.A. de Jager and H. Van As

Laboratory of Biophysics, Wageningen University, De Dreijenlaan 3, 6703 HA Wageningen, The Netherlands

NMR imaging (NMRI or MRI), has proven to be a useful tool to study plant water relationships. NMRI is a non-invasive technique that can be used to measure a number of different physical parameters. These parameters can be related directly to tissue water content, average cell size, cell water membrane permeability. In addition, MRI allows to measure quantitatively water transport<sup>1,2</sup>.

In the study of plant water relationships two types of MRI measurements are of special interest. The first is multi-echo (ME) MRI<sup>1</sup>. This type of experiment can be used to calculate two parameters for every pixel in an image, amplitude and a relaxation time,  $T_2$ . The amplitude parameter is directly related to the amount of water per pixel, and thus to tissue water content. The second parameter,  $T_2$ , is strongly correlated to vacuole size and membrane permeability<sup>2</sup>.

A second type of measurement, fast dynamic MRI (PFG-RARE)<sup>2</sup>, has enabled the measurement of xylem (and phloem) flow on a per pixel basis in intact plants. This type of experiment yields the distribution of flow velocities for every pixel, from which the average linear flow velocity, the amount of flowing water, and the volume flow per pixel can be calculated. This type of experiments has been used to study embolism induction and repair<sup>3</sup>.

By combining the two types of MRI experiments into a MRI (PFG-ME) experiment data is acquired in such a way that water is first separated on the basis of velocity, after which the relaxation time of water moving at different speeds is determined individually. In this way information is obtained of the vessel dimension in which water flows and the vessel wall permeability.

Measurements on a small eucalyptus tree and on a tomato plant have shown that it is possible to measure, in one experiment, a set of parameters that enable us to a) accurately measure and quantify flow in stems containing different vessel sizes, b) specifically measure characteristics of flowing water, providing qualitative information on the distribution of the sizes of water-conducting vessels, and c) measure characteristics of water in cells surrounding water-conducting vessels, which can be used to provide information on the exchange of water between vessels and surrounding (stationary) water in the cells<sup>4</sup>.

### References

- 1) Van der Weerd *et al.* 2001. *J Exp Bot* 52, 2333
- 2) Scheenen *et al.* 2002. *Biophys J* 142, 481
- 3) Scheenen *et al.* 2002. *Plant Physiol* (submitted)
- 4) Tallarek *et al.* 1999. *J Phys Chem B* 103, 7654.

## Influence of stagnant zones on transient and asymptotic dispersion in macroscopically homogeneous porous media

D. Kandhai<sup>1,2</sup>, D. Hlushkou<sup>3,4</sup>, A. Hoekstra<sup>1</sup>, P. M. A. Sloot<sup>1</sup>, H. Van As<sup>3</sup>, U. Tallarek<sup>3,5</sup>

<sup>1</sup>Section of Computational Science, University of Amsterdam, Amsterdam, The Netherlands

<sup>2</sup>Kramers Lab. of Physical Technology, Delft University of Technology, Delft, The Netherlands

<sup>3</sup>Laboratory of Biophysics and Wageningen NMR Centre, Wageningen University, Dreijenlaan 3, 6703 HA Wageningen, The Netherlands

<sup>4</sup>Max Planck Institute for Dynamics of Complex Technical Systems, Magdeburg, Germany

<sup>5</sup>Lehrstuhl für Chemische Verfahrenstechnik, Otto-von-Guericke Universität Magdeburg, Universitätsplatz 2, 39106 Magdeburg, Germany.

A detailed understanding of transport in porous media over the intrinsic temporal and spatial scales is important in many technological and environmental processes. Natural and industrial materials like soil, rock, filter cakes or catalyst pellets often contain low-permeability zones with respect to hydraulic flow of liquid through the medium or even stagnant regions which remain purely-diffusive. Despite numerous theoretical, experimental and numerical studies the transient and asymptotic behaviour of dispersion in porous media is not completely understood. In particular, the influence of stagnant zones with respect to the actual mesoscopic and macroscopic flow field heterogeneity of the medium has found little attention in theory and experiment.

We have studied diffusion-limited mass transfer (1), transient and asymptotic longitudinal dispersion in single-phase liquid flow through a fixed bed made of spherical, permeable (porous) particles, covering several orders of characteristic time and length scales associated with fluid transport. The observed behavior was contrasted to the corresponding fluid dynamics in a random packing of equally sized impermeable (nonporous) spheres with interparticle void fraction of 0.37. Experimental data for Pe up to 100 were obtained by pulsed field gradient NMR and were complemented by numerical simulations employing a hierarchical transport model with a discrete (lattice-Boltzmann) interparticle flow field using computer generated models of the interparticle pore space (2). Finite-size effects in the simulation associated with the spatial discretization of support particles or the dimension and boundaries of the bed were minimized and the simulation results are in reasonable agreement with experimental results.

We conclude that the intraparticle liquid holdup clearly dominates over contributions caused by the intrinsic flow field heterogeneity and boundary-layer mass transfer.

### References

- 1 Tallarek U, Vergeldt FJ, Van As H. 1999. Stagnant mobile phase mass transfer in chromatographic media: Intraparticle diffusion and exchange kinetics. *J. Phys. Chem. B.* 103: 7654-7664.
- 2 Kandhai D, Tallarek U, Hlushkou D, Hoekstra A, Sloot PMA, Van As H. 2002. Numerical simulation and measurement of liquid hold-up in biporous media containing discrete stagnant zones. *Phil. Trans. R. Soc. Lond. Ser. A* 360: 521-534.

## DARTS: Diffusion and displacement analysis by relaxation time separated PFG NMR

*T. Sibgatullin, P.A. de Jager, F.J. Vergeldt, E. Gerkema and H. Van As*

Laboratory of Biophysics, Wageningen University, Dreijenlaan 3, 6703 HA Wageningen, The Netherlands.

The displacement of molecules in biosystems is an important process to understand the physiological processes at a molecular level. PFG NMR samples the displacement in the gradient direction of an ensemble of molecules over the time  $\Delta$ . An ensemble is a group of molecules that experience a similar environment during  $\Delta$ . If the ensemble is inhomogenous due to compartments separated by (permeable) membranes the measured displacements contain information about the dimension of the compartments. T2 can be used to discriminate different ensembles (1), but the analysis of the T2 decay now becomes critical.

Presented are the results of an integrated STE PFG-T2 study on Apple tissue at 30 MHz. The two-dimensional PFG-T2 dataset is analysed in the following ways to extract the information of the different ensembles. One-dimensional fits with a discrete number (one, two and three) - and a distribution of exponentials with  $D = f(TE)$  and  $T2 = f(G^2)$  followed by the two-dimensional fit giving a more comprehensive presentation.

An IR (T1) preparation module is added to suppress the signals from a specific ensemble to improve the discrimination between the other components.

### References

- (1) van Dusschoten D, Moonen CT, de Jager PA, Van As H. (1996) Unraveling diffusion constants in biological tissue by combining Carr-Purcell-Meiboom-Gill imaging and pulsed field gradient NMR. *Magn Reson Med* 36:907-913.

## Structural Genomics: Methods for fast screening and structure determination by NMR

*B. van Buuren, J. Dubuc, G.Folkers, L.Koharudin, R. Boelens and R. Kaptein*

The goal of Structural Genomics is to generate three-dimensional structures for the large number of gene products of DNA sequences that are currently becoming available. From this database of structures, information about the function of gene products can then be obtained with the aid of bioinformatics. NMR can determine structures of protein domains and has the potential to become one of the key-players in Structural Genomics. However, there still exist some bottlenecks, such as high-throughput protein, production, fast and robust protocols for screening and data-analysis. Important elements of the project are expression of large quantities of suitable proteins for NMR spectroscopy and setting up efficient protocols for screening, data recording and structure calculation. Here we show the preliminary results of our Structural Genomics efforts.

## Using liquid state $^{31}\text{P}$ NMR to characterize P forms in P enriched sandy soils

*G.F. Koopmans, W.J. Chardon, and P. van der Meer*

In areas with intensive agriculture, soil phosphorus (P) contents have increased due to high application rates of animal manure and/or P fertilizer. These soils are likely to contribute to P enrichment and eutrophication of surface waters. In soil, P is distributed among various inorganic and organic P forms differing in availability for plant uptake and potential for leaching to the environment. To increase our understanding of P availability and mobility, it is, therefore, necessary to study the distribution of P among these forms. Recently, liquid state  $^{31}\text{P}$ -Nuclear Magnetic Resonance (NMR) spectroscopy, a relatively simple and direct technique, has been used to characterize P. In this study, P forms are characterized by  $^{31}\text{P}$ -NMR in alkali extracts of sandy soils treated with different animal manures and N(P)K fertilizers.

## A high-resolution NMR study of long-lived water molecules in both oxidation forms of a bacterial cytochrome c

*Ilaria Bartalesi, Ivano Bertini, Kaushik Ghosh, Antonio Rosato and Paul R. Vasos*

The identification and characterization of water molecules interacting with the polypeptide chain of *B. pasteurii* cytochrome c is reported, based on 2D heteronuclear NMR experiments designed to selectively excite water magnetization, allow for magnetization transfer during the mixing time and record signals from amide protons after suppression of the water signal.

The resulting signals are thus only the HSQC resonances belonging to amide protons to which water magnetization has been transferred during the mixing time. The aim is to differentiate protons to which magnetization is transferred mainly through nOe effect from protons that are influenced mainly by chemical exchange with water.

Internal water molecules with long exchange times have a distinct behavior from that of hydration water molecules and their position can be inferred from the spectral information. The structural water molecules have long residence times and, as a consequence, appear in analogous positions in the crystal structure and in the NMR experiments; their position is important for the stability of the protein fold and implicitly for the protein function.

---

**SON NMR Large-Scale Facility for Biomolecular NMR, Utrecht**

*Nico van Nuland and Rainer Wechselberger*

Started in 1994 as a collaboration between Utrecht University and the Netherlands Foundation for Chemical Research (SON) and with financial support of the European Union, the Utrecht NMR Large-Scale Facility (SONNMRLSF) is providing access and support for research in Biomolecular NMR to academic and industrial researchers from the European Union (EU) and Associated States.

---

**NMR-Solution structure of the *Thermotoga maritima* ribosomal protein L11**

*Sergey Ilin, Aaron Hoskins, Harald Schwalbe, Jens Wöhnert*

The NMR-solution structure of the full-length ribosomal protein L11 from the thermophilic bacterium *Thermotoga maritima* in its unbound form will be presented. The comparison of the solution structure of the free protein with the structure of the RNA-bound protein indicates a role of domain reorientation in the process of RNA-binding.

## H-bonding features in two redox states between the isoalloxazine ring and the protein moieties of flavodoxin from *Desulfovibrio vulgaris*.

*Gary N. Yalloway, Frank Löhr, Hans Wienk, Andrea Hrovat, Martin Knauf, Stephen G. Mayhew and Heinz Rüterjans*

Uniformly labelled  $^{15}\text{N}$  and  $^{15}\text{N}/^{13}\text{C}$  labelled recombinant flavodoxin from *D. vulgaris* was expressed in *E. coli* TG1. The hydroquinone was formed by the addition of an excess of sodium dithionite. Unambiguous assignment of backbone resonances (HN, N, CO and Ca) was obtained for all residues in the reduced state. Sidechain assignment was accomplished for 100 % of the aliphatic  $^{13}\text{C}$  atoms. The assignment for the fully reduced form of the protein revealed significant changes around the flavin binding site when compared to the oxidized protein.

Recent developments in modern pulse sequences have made it possible to detect H-bonds using scalar couplings [1]. Hydrogen bonding plays a major role in the tight binding of the flavin mononucleotide (FMN) co-factor in flavodoxins. The present NMR investigation provides direct experimental evidence for  $^1\text{H}-^{31}\text{P}$  and  $^{15}\text{N}-^{31}\text{P}$  scalar couplings involving the phosphate moiety, also intermolecular H-bonds  $^{2h}\text{J} (^{15}\text{N}, ^{15}\text{N})$  couplings between the nitrogen atoms of the isoalloxazine ring and the protein backbone. The hydrogen bond interactions between the flavin co-factor and the apoprotein of flavodoxin in the reduced state were compared to the oxidized state [2] to establish whether changes in the hydrogen bonding network play a key role in the regulation of redox properties in flavodoxin.

### References

1. Grzesiek, S., Cordier, F. and Dingley, A. J. (2001) *Methods in Enzymology* 238, 111-133
2. Löhr, F., Mayhew, S. G. and Rüterjans, H. (2000) *J. Am. Chem. Soc.* 122, 9289-9295

## NMR Solution Structure of G-quadruplex of d(G4T4G3)2

*Martin Èrnugelj and Janez Plavec*

DNA and RNA can form structures containing more than two strands. For example, telomeres, the protein-DNA complexes located at the ends of chromosomes, contain guanine-rich repeat sequences that form G-quartets in vitro. This has led to much speculation concerning the possible roles of G-quadruplexes in chromosome replication and maintenance, which has in turn made G-quadruplexes a target for anti-cancer drug design.

Here we report NMR structural studies of d(G4T4G3), a sequence that can be considered an intermediate perturbation between d(G4T4G4) and d(G3T4G3). d(G4T4G3)2 forms an asymmetric dimeric diagonally looped G-quadruplex structure in the presence of  $\text{Na}^+$  ions, which consists of three G-quartet planes and an additional two guanine nucleotides that reside on one side of the G-quadruplex core. The two thymine loops adopt different conformations, and the whole structure is significantly different from the structures formed by the closely related sequences d(G4T4G4) and d(G3T4G3) under similar solution conditions. The cation-dependent folding of the d(G4T4G3)2 quadruplex structure is also distinct from that observed for similar sequences. While both d(G4T4G4) and d(G3T4G3) form bimolecular diagonally looped G-quadruplex structures in the presence of  $\text{Na}^+$ ,  $\text{K}^+$  and  $\text{NH}_4^+$  ions, we have only observed this folding to be favored for d(G4T4G3) in the presence of  $\text{Na}^+$ , but not in the presence of  $\text{K}^+$  or  $\text{NH}_4^+$  ions.

---

List of authors

Adani F. P63  
Akerud T. P13  
Akke M. P13  
Amzel M.L. P68  
Anastasiadis-Pool A. P1  
Antonkine M.L. P2  
Arantes E.C. P66  
Arnesano F. P3, P22, P67  
Assfalg M. P4, P27  
Badora A. L18, P5  
Balatri E. P22  
Balbach J. P6  
Banci L. P3, P19, P20, P22, P27, P44, P67  
Baran M.C. L5  
Barbieri R. P7  
Barker P. P8  
Barsukov I. P9  
Bartalesi I. P10, P76  
Battaini G. P4  
Bauer J. L10  
Bayer E. P11  
Bayer P. P11  
Bentrop D. P12  
Bernado P. P13  
Bernhard F. P14  
Bertini I. L1, P3, P4, P7, P10, P15, P20, P22, P27, P28, P29, P44, P54, P55, P67, P76  
Bisio A. P34  
Blezer E. L10  
Bodiguel J. P19  
Boelens R. P17, P36, P40, P42, P43, P50, P56, P74  
Boetzel R. L21, P16  
Bonvin A.M.J.J. P17, P42, P68, P69  
Bottomley M. L24  
Bratsos I. P18  
Brok H. L10  
Brown K.A. P19  
Bruhn H. P35  
Budinska J. P48  
Buurman P. L18, P5, P25  
Callaghan J. L23  
Cantini F. P20, P22, P27  
Casares S. P21, P24  
Casu B. P34

---

List of authors

Cavazzini D. L17  
Chardon W.J. P75  
Ciofi-Baffoni S. P22  
Clarke A.R. P61  
Collins E. P23  
Collins E.S. P16, P49  
Conejero-Lara F. P21, P24  
Conte P. P25  
Cordopatis P. P26, P68  
Covarrubias M. P12  
Cramaro F. P27  
Craven J. P61  
Crescenzi O. P56  
Critchley D. P9  
D'Amelio N. P31, P70  
Dardel F. L15  
de Jager P.A. L18, P5, P37, P63, P71, P73  
de Waard P. L12, P59  
Del Bianco C. P28  
Del Conte R. P22, P27  
Deraos S. P69  
Derix N.M. P50  
Desvaux H. L11  
Díaz-Orejas R. P40  
Dijkema C. L16, P37  
Doetsch V. L8  
Dolderer B. P28  
Dominguez C. P17  
Donaire A. P39  
D'Onofrio M. P22, P27  
Dubuc J. P74  
Echner H. P28  
Ellis J. P9  
Èrnugelj M. P80  
Fakler B. P12  
Felli I.C. P44  
Fiegig K. L19, P38  
Folkers G. P43, P74  
Fragai M. P29, P55  
Franzoni L. L17, P58, P66  
Fromme P. P2  
Fuchs P. P69  
Fushman D. P30

---

List of authors

Gaggelli E. P31, P70  
Gaggelli N. P31, P70  
Galanis A. P26  
Ganslmeier B. L6  
Garcia de la Torre J. P13  
Garoufis A. P32  
Gelis I. P57  
Georgakopoulos A. P37  
Gerkema E. P73  
Gerotheranassis I. P26, P68, P69  
Ghosh K. P10, P76  
Gnezda K. L16  
Golbeck J.H. P2  
Gonnelli L. P22  
Grabner A.R. P12  
Griesinger C. P62  
Groetzinger J. L20, P35, P52  
Gronwald W. L6  
Grundstrom T. L13  
Guerrini M. P34  
Guiberman E. P11  
Günther U. P33  
Haase A. L7  
Habeck M. L25  
Hadjiliadis N. P32  
Hall J.F. P39  
Hart B. L10  
Hartmann H.-J. P28  
Hasnain S.S. P39  
Hecht O. P35  
Heeminga M.A. P25  
Hellingwerf K.J. P50  
Hirai K. P23  
Hlushkou D. P72  
Hoekstra A. P72  
Hollender D. P41  
Hore P.J. P7  
Hoskins A. P78  
Houben K. P36  
Hounslow A.M. P61  
Hricovini M. P34  
Hrovat A. P79  
Huang Y.J. L5

---

List of authors

Ilin S. P78  
Iordanidis A. P37  
Jacobs D. L19, P38  
Jamart-Grégoire B. P19  
James R. L21, P16, P49  
Jiménez B. P39  
Jordan P. P2  
Kabel M.A. L12  
Kalbitzer H.R. L6  
Kalodimos C. P43  
Kamphuis M.B. P40  
Kandhai D. P72  
Kaptein R. L3, P42, P43, P50, P74  
Katsaros N. P18, P53, P57  
Katsemi V. P47  
Kirchhöfer R. L6  
Kiss T. P41  
Klammt C. P14  
Kleanthous C. L21, P16, P46  
Knauf M. P79  
Koharudin L.M.I. P42, P74  
Koopmans G.F. P75  
Kopke Salinas R. P43  
Kowalewski J. L14  
Krauss N. P2  
Krippahl L. P44  
Kruk D. L14  
Kubicek K. P44  
Lamosa P. P45  
Larsson G. L13  
Laue E.D. L23  
Le Duff C. P46  
Leippe M. P35  
Lipta T. P48  
Liu Z. L24  
Löhr F. P47, P79  
Lombardi V. P48  
Lopez-Mayorga O. P21, P24  
Luchinat C. P4, P7, P28, P29, P41, P54, P55, P57  
Lücke C. L17, P66  
Luyten I. L24  
Macdonald C.J. L21, P49  
Majer E. P48

---

List of authors

Mancini F. P70  
Manessi-Zoupa E. P26  
Mangani S. P22  
Marhuenda-Egea F. P22  
Marks D.R.A. P50  
Martinez J.C. P21  
Matsoukas J. P69  
Mayhew S.G. P79  
McDermott A. L22  
Messias A.C. L24  
Molinari H. P60  
Molteni E. P31, P70  
Monaco H. P60  
Montelione G.T. L5  
Moore G.R. L21, P16, P46, P49  
Moratal J.-M. P39  
Moseley H.N.B. L5  
Mott H.R. L23  
Moura J.J.G. P44  
Moussa S. L6  
Mouzopoulou B. P18  
Muller R.N. P51  
Murzina N.V. L23  
Myari A. P32  
Nassar A. L6  
Neidig K.-P. L6  
Nerinovski K. P7, P41, P55  
Nicolay K. P64  
Nielsen P.R. L23  
Nietlispach D. L23  
Nilges M. L25  
Nilsson T. L14  
Oyama Jr. S. P66  
Pachta-Nick M. L20, P52  
Padrta P. P65  
Pairas G. P26  
Papakyriakou A. P18, P53  
Parigi G. P54, P55  
Patel B. P9  
Penfold C. L21, P49  
Pertinhez T.A. P66  
Piccioli M. P57  
Piccolo A. P25

---

List of authors

Pickart C. P30  
Picone D. P56  
Pierattelli R. P7, P8, P19, P26  
Plavec J. P80  
Poggi L. P57  
Pons M. P13  
Povilaityte V. L12  
Prescot A. P9  
Pristovšek P. P58, P66  
Pukalskas A. L12, P59  
Ragona R. P60  
Ratcliffe R.G. L9  
Reed M.A.C. P61  
Richter C. P62  
Rieping W. L25  
Roberts G.C.K. P9  
Rocha P. P46  
Rosato A. P10, P22, P44, P67, P76  
Rossi G.L. L17  
Ruiz-Dueñas F.J. P22  
Rüterjans H. L2, L17, P14, P33, P47, P58, P66, P79  
Saarikettu J. L13  
Sadqi M. P21, P24  
Sahato G. L5  
Santos H. P45  
Sattler M. L24  
Saxena K. L19, P38  
Scaglia B. P63  
Schepers J. P64  
Schininà E. P66  
Schleucher J. L13  
Schwalbe H. P1, P23, P62, P78  
Segawa S. P23  
Selenko P. L24  
Serber Z. L8  
Shipp E.L. P20  
Shirasu K. P46  
Shirokov V. P14  
Sibgatullin T. P73  
Sklenar V. P65  
Sloot P.M.A. P72  
Snyder D. L5  
Spisni A. L17, P66

---

List of authors

Sprangers R. L24  
Spyroulias G.A. P26  
Stefl R. P65  
Stehlik D. P2  
Stier G. L24  
Stopar D. L16  
Su X.C. P67  
Sveshnikova N. L13  
Tallaker U. P72  
Tambone F. P63  
Tancredi T. P56  
Tejero R. L5  
Thiru A. L23  
Thompsett A.R. P3, P22  
Tisé C. L15  
Tomaselli S. P56  
Torri G. P34  
Tozawa K. L21, P49  
Trenner J. L6  
Trojanis A. P26, P68, P69  
Troncone A. P48  
Tselios T. P69  
Turano P. P4, P10, P27  
Turner D.L. P45  
Tzakos A. P26, P68, P69  
Ugolini R. P60  
Valensin D. P31, P70  
Valensin G. P31, P70  
Valentine J.S. P20  
Van As H. L4, P71, P72, P73  
van Beek T.A. P59  
van Buuren B. P74  
van der Horst M.A. P50  
van der Meer P. P75  
van Lagen B. L18, P5, P25, P37  
van Nuland N. L20, P21, P24, P48, P50, P52, P68, P69, P77  
Vanarotti M. P10  
Varadan R. P30  
Vasile F. P60  
Vasos P.R. P27, P76  
Veeken A. P63  
Venskutonis P.R. P59  
Vergeldt F.J. P71, P73

---

List of authors

Viezzoli M.S. P27, P67  
Voelter W. P28  
Vogtherr M. L19, P38  
von der Heyden C. P62  
Walker O. P30  
Waltho J.P. P61  
Wechselberger R.W. L20, P46, P48, P52, P56, P77  
Weser U. P28  
Wienk H. P79  
Wijmenga S.S. L13  
Windt C.W. P71  
Wirmer J. P23  
Wöhnert J. P78  
Yalloway G.N. P79  
Zanier K. L24  
Zdunek J. L13  
Zeeb M. P6  
Zetta L. P60  
Zidek L. P65